

METHOD

Using mobile acoustic monitoring and false-positive N-mixture models to estimate bat abundance and population trends

Bradley J. Udell¹  | Bethany Rose Straw¹ | Susan C. Loeb² |
 Kathryn M. Irvine³  | Wayne E. Thogmartin⁴ | Cori L. Lausen⁵ |
 Jonathan D. Reichard⁶ | Jeremy T. H. Coleman⁶  | Paul M. Cryan¹ |
 Winifred F. Frick^{7,8} | Brian E. Reichert¹ 

¹US Geological Survey, Fort Collins Science Center, Fort Collins, Colorado, USA

²United States Forest Service, Southern Research Station, Clemson, South Carolina, USA

³US Geological Survey, Northern Rocky Mountain Science Center, Bozeman, Montana, USA

⁴US Geological Survey, Upper Midwest Environmental Sciences Center, La Crosse, Wisconsin, USA

⁵Wildlife Conservation Society Canada, Toronto, Ontario, Canada

⁶United States Fish and Wildlife Service, Ecological Services, Hadley, Massachusetts, USA

⁷Bat Conservation International, Austin, Texas, USA

⁸Ecology and Evolutionary Biology, University of California, Santa Cruz, California, USA

Correspondence

Bradley J. Udell

Email: budell@usgs.gov

Handling Editor: Lydia Beaudrot

Abstract

Estimating the abundance of unmarked animal populations from acoustic data is challenging due to the inability to identify individuals and the need to adjust for observation biases including detectability (false negatives), species misclassification (false positives), and sampling exposure. Acoustic surveys conducted along mobile transects were designed to avoid counting individuals more than once, where raw counts are commonly treated as an index of abundance. More recently, false-positive abundance models have been developed to estimate abundance while accounting for imperfect detection and misclassification. We adapted these methods to model summertime abundance and trends of three species of bats at multiple spatial scales using acoustic recordings collected along mobile transects by partners of the North American Bat Monitoring Program (NABat) from 2012 to 2020. This multiscale modeling spanned individual transect routes, larger NABat grid cells (10 km × 10 km), and across the entire extent of modeled species ranges. We estimated relationships between species abundances and a suite of abiotic and biotic predictors (landcover types, climatological variables, physiographic diversity, building density, and the impacts of white-nose syndrome [WNS]) and found varying levels of support between species. We present clear evidence of substantial declines in populations of tricolored bats (*Perimyotis subflavus*) and little brown bats (*Myotis lucifugus*), declines that corresponded in space and time with the progression of WNS, a devastating disease of hibernating bats. In contrast, our analysis revealed that similar population-wide declines probably have not occurred in big brown bats (*Eptesicus fuscus*), a species known to be less affected by WNS. This study provides the first abundance-based species distribution predictions and population trends for bats in their summer ranges in North America. These models will probably be applicable to assessing

This is an open access article under the terms of the [Creative Commons Attribution-NonCommercial](https://creativecommons.org/licenses/by-nc/4.0/) License, which permits use, distribution and reproduction in any medium, provided the original work is properly cited and is not used for commercial purposes.

Published 2024. This article is a U.S. Government work and is in the public domain in the USA. *Ecological Monographs* published by Wiley Periodicals LLC on behalf of The Ecological Society of America.

wildlife populations in other monitoring programs where acoustic data are used or where false-negative and false-positive detections are present. Finally, our abundance framework (as a spatial point pattern process) can serve as a foundation from which more sophisticated integrated species distribution models that incorporate additional streams of monitoring data (e.g., stationary acoustics, captures) can be developed for North American bats.

KEYWORDS

bat conservation, disease, echolocation, *Eptesicus fuscus*, imperfect detection, *Myotis lucifugus*, NABat, North American Bat Monitoring Program, *Perimyotis subflavus*, unmarked, white-nose syndrome, wildlife

INTRODUCTION

Bat populations in North America are under threat from habitat destruction, land use change, climate change, wind energy, and the spread of invasive pathogens and diseases such as white-nose syndrome (WNS) (Cheng et al., 2021; Frick et al., 2020; Friedenberg & Frick, 2021; O'Shea et al., 2016; Sherwin et al., 2013). In the face of such threats, the North American Bat Monitoring Program (NABat)—a partner-driven, multiagency, international network—was developed to address historical limitations in bat monitoring, with a mission to support collaborative monitoring of bat species across North America and deliver information on the status and trends of bats across their ranges (Loeb et al., 2015; Reichert et al., 2021). Results from NABat monitoring efforts inform conservation decision-making to support the long-term viability of bat populations across the continent (Loeb et al., 2015). Given the complex and varied life histories of bats in North America, diverse monitoring techniques across seasons are needed to understand the status and trends of bat populations (O'Shea et al., 2004; O'Shea & Bogan, 2003).

To date, most population impact assessments for bats have been based on abundance estimates from counts of bats in winter roost sites (winter colony counts) or estimates of bat occupancy and/or activity during the summer active season using acoustic sampling or live-capture data. For example, winter colony abundance of three species of hibernating bats (little brown bats, *Myotis lucifugus*; tricolored bats, *Perimyotis subflavus*; and northern long-eared bats, *Myotis septentrionalis*) have declined by more than 95% wherever WNS has occurred (Cheng et al., 2021). Declines corresponding with WNS have also been documented for these species in analyses of summer occupancy and activity rates derived from acoustic monitoring data (e.g., Straw et al., 2022; Udell et al., 2022). Northern long-eared bats have been listed as endangered in the United States (US Fish and Wildlife Service, 2022a) and tricolored bats have been proposed for listing under the US Endangered Species Act

(US Fish and Wildlife Service, 2022b). At the time of this writing, the status of little brown bats is being reviewed for potential listing under the US Endangered Species Act (US Fish and Wildlife Service, 2022). All three species were emergency listed as endangered in Canada under the federal Species at Risk Act in 2014 (Environment and Climate Change Canada, 2018). However, little is currently known about bat abundance in their summer distributions including their spatial and temporal trends. Rectifying this historical knowledge gap during the summer maternity season (a critical period for bat demography) would allow for more informed population conservation and management decisions. Acoustic monitoring in the summer shows promise for monitoring bat population trends across entire species ranges, as this is the season when bats are most active and dispersed across the diverse landscapes they inhabit.

Acoustic monitoring via automated recording units is most often conducted at stationary points (Hayes et al., 2009) where a “detection” is defined as a series of echolocation pulses associated with a single pass of a bat near an ultrasonic microphone. To date, no method exists for distinguishing unique individuals from multiple detections at stationary recording stations. Mobile acoustic transect surveys, or acoustic sampling for bats while driving along predetermined routes, were developed specifically to overcome this limitation (Britzke & Herzog, 2009; Roche et al., 2005; Roche et al., 2011). Inferences drawn from mobile acoustic transect surveys often assume that each acoustic detection corresponds to a single bat given the travel speed of a vehicle (at least 32 km/h, which is faster than most species of bats typically fly, Hayward & Davis, 1964; Patterson & Hadin, 1969). The resulting counts of bat detections are treated as a raw index of relative abundance to infer trends over time and are typically analyzed with the use of generalized linear mixed models (Braun de Torrez et al., 2017; D'Acunto et al., 2018; Evans et al., 2021; Roche et al., 2011; Simonis et al., 2020; Whitby et al., 2014). Whereas this approach can incorporate observation-level

covariates to adjust expected counts for observation bias (i.e., false negatives, Barker et al., 2018; Evans et al., 2021), it is unlikely to adequately account for the combination of negative and positive biases from separate processes such as imperfect detection (false negatives) and species misclassification (false positives). These directional biases are likely to vary in different ways across sampling nights, years, and locations. Thus, trends inferred from such indices may be unreliable (e.g., Anderson, 2001; Miller et al., 2015). However, shortcomings might be overcome by simultaneously modeling both observation processes (detectability and misclassification), along with the ecological process (abundance), while accounting for important sources of variation in each.

NABat guidance for mobile acoustic transects stresses the importance of conducting multiple temporally replicated surveys during the maternity season each year to facilitate analysis and more reliable inferences using unmarked abundance methods (Loeb et al., 2015). Unmarked abundance models such as the N-mixture model (Royle, 2004) allow for inference to abundance while accounting for detectability; however, until recently, there were no formulations of N-mixture models that were robust to false-positive detections from species misclassification (DiRenzo et al., 2019). False-positive N-mixture models (e.g., Clare et al., 2021; Clement et al., 2022; Doser et al., 2021) have now been developed to overcome this limitation by building upon the rich literature of false-positive occupancy models for species misidentification (e.g., Banner et al., 2018; Chambert et al., 2015; Chambert, Waddle, et al., 2018; Kéry & Royle, 2020; Miller et al., 2011; Royle & Link, 2006; Stratton et al., 2022; Wright et al., 2020). For example, Doser et al. (2021) built upon the single-species methods of Chambert, Waddle, et al. (2018) to develop a false-positive N-mixture model for ambiguous count data by also incorporating a hypergeometric observation model for a subset of manually reviewed data. Clement et al. (2022) extended work by Chambert, Grant, et al. (2018) to develop a false-positive N-mixture model that relies on parameter constraints rather than a subset of manually reviewed data to estimate parameters.

In theory, unmarked abundance models provide inferences on absolute abundance, but only when model assumptions (e.g., population closure, no unmodeled heterogeneity, no sampling bias) are fully met. While several field evaluations of N-mixture models have reported reasonable population estimates compared with those from more rigorous sampling methods (e.g., Bötsch et al., 2020; Costa et al., 2020; Ficetola et al., 2018), simulation studies have demonstrated that estimates of absolute abundance are sensitive to assumption violations (e.g., Link et al., 2018). Thus,

inferences from unmarked abundance models are best treated as those pertaining to relative abundance (i.e., covariate effects, proportional trends over time, population growth rates, demographic rates, etc.; Barker et al., 2018; DiRenzo et al., 2019; Farr et al., 2022; Link et al., 2018). In this study, we adapted the false-positive abundance methods of Doser et al. (2021) to estimate the relative abundance of bats using data collected during mobile acoustic transect surveys. After simplifying their observation model for ambiguous counts from a hurdle distribution to a Poisson distribution, the resulting model was identical to the single-species observation model described by Clement et al. (2022); but it also retained the hypergeometric observation model from Doser et al. (2021) which let us use a subset of manually reviewed and confirmed observations to estimate false-positive and average detection rates without assuming parameter constraints.

Using this single-species approach, we analyzed mobile acoustic data from the NABat database for three bat species of varying levels of conservation concern. We provide the first-ever “summer abundance status and trends” analysis for these species at multiple spatial resolutions (transects, 10 km × 10 km grid cells, and across the extent of each species range for which there are adequate monitoring data [i.e., the “modeled species range”]). We also estimated the effects of relevant abiotic and biotic predictors of abundance at landscape scales (e.g., WNS impacts across the winter distribution) and provided maps of relative abundance distributions and trends over time for each species. These methods are generally applicable to other systems where modeling abundance (or relative abundance) is of primary interest, and the observation process is prone to biases from both imperfect detection and false positives (e.g., most monitoring methods that rely on automated classification processes, such as acoustic monitoring, environmental DNA, and camera trapping).

MATERIALS AND METHODS

Sampling methods for mobile transect acoustics

NABat’s mobile transect sampling protocols are fully described in Chapter 5 of Loeb et al. (2015) and the NABat mobile transect standard operating procedures (Martin et al., 2022a, 2022b, 2022c). Briefly, NABat grid cells (10 km × 10 km, Talbert & Reichert, 2018) are sampled using ultrasonic acoustic detectors while driving along transect routes on roads. A generalized random tessellation stratified (GRTS) sampling approach (Stevens &

Olsen, 2004) was used to select NABat cells whenever possible and ensured that sampled locations were spatially balanced; however, data were accepted from all NABat contributors including legacy monitoring programs that predated NABat guidance (see Appendix S1 for more information on exceptions). Spatially balanced sampling designs help to ensure that the distribution of potential environmental correlates at sampled grid cells are representative of their distribution across the species' range (Stevens & Olsen, 2004).

Transect routes were selected based on the feasibility and safety of maintaining a vehicle speed of 32 km/h (20 miles/h) throughout a sampling event. Recommended route lengths were between 25 and 48 km to ensure that grid cells were adequately sampled; however, transects that spanned multiple grid cells were divided between grid cells, which produced some transect lengths shorter than 25 km. Routes were driven at least twice, typically within 1 week during maternity season (prevolancy, i.e., before the newborn of year can fly) although sometimes partners conducted many additional surveys throughout the summer. The NABat Partner Portal project identifier (project ID), detector type, and microphone type were also recorded for each acoustic file, and consistency of hardware types and settings among and within years was encouraged (Loeb et al., 2015).

Acoustic files were classified to species level using automated call-detection and call identification (auto ID) software (e.g., several versions of "Sonobat," "Wildlife Acoustics Kaleidoscope," and "Bat Call Identification, BCID 2.7d"). Auto IDs and the software used to produce them were then recorded. Although the NABat protocol recommends that all auto IDs from mobile transect surveys be manually reviewed (Reichert et al., 2018), practical constraints often led to only a subset of high-quality files being reviewed. For each reviewed file, the manually classified species identification (manual ID) was recorded and linked with the corresponding auto ID. The full protocol for manual review of acoustic files is documented in Reichert et al. (2018). For this analysis, we tracked the total number of auto IDs each sampling night that were manually reviewed, and of those, the number that was also confirmed as the species of interest (auto ID = manual ID).

NABat database and contributors

We accessed mobile transect acoustic data through the NABat data request process in September 2022 (<https://www.nabatmonitoring.org/get-data>; NABat, 2021, 2022). The compiled dataset represents contributions from 55 individual NABat Partner Portal projects. Data included nightly summaries of the total number of auto IDs for

each species given the software type, along with the total number of files that had been reviewed and confirmed as the species of interest. Individual records for the auto ID of each acoustic file were linked to the project ID (thereby maintaining provenance and distinguishing efforts), NABat grid cell, route ID, route length, software type, detector type, sampling night, and manually reviewed information (i.e., if a file was reviewed, to which species it was manually classified). Data were cleaned and processed for analysis using the workflow described in Appendix S1.

Species of interest and scope of inference

We focused our analyses on three species of hibernating bats: tricolored bats, little brown bats, and big brown bats (*Eptesicus fuscus*). These species were selected based on conservation concerns and data availability, with adequate levels of monitoring effort and species detections dating back through 2012. Northern long-eared bats were also considered but not included due to an insufficient number of detections. Following Loeb et al. (2015), the scope of inference for abundance was based on the prevolancy of the summer season each year, meaning the population of interest does not include bats born in the same summer that the data were collected. This period was defined for this analysis as 1 May to 15 July, noting the data were not uniformly distributed between these starting and ending dates by location. In most cases, the first mobile transects of the summer were conducted in late May or June but monitoring sometimes began in early May in southern regions. Although such data were rare, we also included data from the postvolancy period (defined as 16 July to 28 August) but assumed the population was open between the prevolancy and postvolancy periods by estimating a different population abundance for the prevolancy and postvolancy seasons each year. This was included to account for changes in the population that would otherwise violate the assumption of population closure, for example, when newborns of the year become available for sampling. Because mobile transect sampling did not span the entire published range of any species, the spatial scope of inference was bounded to the "modeled species range" that we defined as the geographic region for which there was adequate monitoring data to support predictions. This modeled range was determined separately for each species by fitting a spatial kernel around all locations with at least one positive species detection and thresholding above a minimum value. We chose the thresholding value for each species that was as high as possible to minimize the effective

buffer distance around the monitoring data, while also low enough to avoid large holes in the predicted distribution. The modeled range of the tricolored bat (3,524,744 km²) represented ~63% of the defined geographic range (5,623,669 km²). For little brown bats, the modeled range of (5,163,527 km²) represented ~43% of the defined geographic range (12,040,700 km², National Atlas of the United States, 2011); and for big brown bats, the modeled range of (4,925,449 km²) represented ~40% of the defined geographic range (12,289,473 km², National Atlas of the United States, 2011). For little brown bats and big brown bats, two separate regions (East and Northwest) were designated based on the availability/accessibility of hibernacula and winter monitoring data (e.g., Weller et al., 2018, which was used as a predictor of summer abundance, see our *Materials and methods: Predictive covariates: Linking winter and summer populations and quantifying WNS impacts* section). For little brown bats, the inclusion of separate regions was also considered due to potential differences in species behavior (Blejwas et al., 2023).

Basic modeling framework for estimating abundance

The goal of single-species, false-positive N-mixture models (Clement et al., 2022; Doser et al., 2021) is to estimate detection rates, false-positive rates, and animal abundances (and/or occupancy; e.g., Clement et al., 2022) given temporally replicated counts and additional information such as a subset of counts that are manually reviewed, parameter constraints, or strong Bayesian priors. In the following sections, we first describe the abundance model for NABat grid cells as an inhomogeneous point process (e.g., Fletcher et al., 2019). Next, we describe the spatially varying thinning process on grid cell abundance that adjusts for the partial survey effort using a mobile transect and accounts for differences in abundance between transects and grid cells based on the transect length in each. Then, we present the observation model that accounts for imperfect detection and misclassification bias. Given that the NABat protocol includes a manual review process for auto IDs (Reichert et al., 2018), we focused on a method that could estimate parameters directly from auto ID count data and a subset of manually reviewed records (e.g., Doser et al., 2021). This approach had the additional benefits of (1) directly downgrading auto IDs in the observation model that were classified as false positives, (2) providing further information to estimate conditional latent abundance states, and (3) avoiding biases that arise from imposing strong parameter constraints (or priors) when they are too restrictive for the modeled system. Last, we detail how we included covariates and

random effects to explain and account for heterogeneity in abundance, average detection rates, and false-positive rates; this formulation was an attempt to make our model robust to heterogeneity in all aforementioned parameter assumptions.

General abundance model

We modeled latent abundance in each grid cell and time period (year × season) N_{it} based on a Poisson point pattern process:

$$N_{it} \sim \text{Poisson}(\lambda_{it}). \tag{1}$$

The expected abundance of individuals at each grid cell i each time period t (λ_{it}) is modeled as a function of spatial (grid cell), temporal (season, year), and spatiotemporal (grid cell and year) covariates:

$$\log(\lambda_{it}) = \beta_0 + \sum_{k=1}^K \beta_k \times x_{it}^k, \tag{2}$$

where β_0 is the overall intercept (the average grid cell abundance in the prevolancy season in year 1), x_{it}^k denotes covariate k at grid cell i and time period t with β_k coefficients (i.e., covariate effects). Note that, while the notation x_{it}^k is used for generality, purely temporal covariates would be constant in the i 'th dimension, while purely spatial covariates are constant in the t 'th dimension.

Transect abundance model

One of the primary challenges in estimating abundance is accounting for the area that has been sampled by transects (sampling exposure), both with respect to other transects (differential sampling effort) and with respect to the NABat grid cell (i.e., what proportion of animals in each grid cell were exposed to sampling). While transect length is commonly used as an offset or covariate on total bat activity (i.e., expected number of detections), extending the same logic to predict transect abundance within a grid cell is problematic. First, because the unique area sampled along a transect is bounded by the area of the grid cell (and similarly, abundance along a transect is bounded by the grid cell abundance), the relationship between transect length and transect abundance should be increasing but saturating (e.g., Royle et al., 2007). Second, when it comes to making predictions at the grid cell level, because transect length is only a proxy of sampled area, it is unknown which value for transect length would correspond to the same area of a grid cell (100 km²).

Following work by Royle et al. (2007) and others (e.g., Kéry & Royle, 2015), we used an inverse transect length covariate to account for differential sampling exposure and to explicitly link transect-level and grid cell-level abundances. Using this approach, we denote N_{it} as the grid cell-level abundance, M_{it} as the transect-level abundance, and $\phi(\text{TL}_i)$ as the average sampling exposure (i.e., nonrandom availability, the proportion of animals in a grid cell that may be encountered along a transect) of M_{it} within N_{it} based on the transect length (TL_i). We note that, because bats are highly vagile animals, both M_{it} and N_{it} correspond to the total number of bat home ranges intersecting each spatial extent each time period. By assuming that $M_{it} \sim \text{Binomial}(N_{it}, \phi_i(\text{TL}_i))$, $\phi_i(\text{TL}_i) = \exp\left(-\frac{\beta_{\text{TL}}}{\text{TL}_i}\right)$, and $\beta_{\text{TL}} > 0$, the marginal distribution for μ_{it} (the expected value of M_{it}) can be modeled $\lambda_{it} \times \phi_i(\text{TL}_i)$. This arrangement can be formulated as a single log link by adding the expression $-\frac{\beta_{\text{TL}}}{\text{TL}_i}$ to the log link in Equation (2), which we used as our estimating equation for transect-level abundance M_{it} :

$$M_{it} \sim \text{Poisson}(\mu_{it}), \quad (3)$$

$$\log(\mu_{it}) = \beta_0 + \sum_{k=1}^K \beta_k \times x_{it}^k - \frac{\beta_{\text{TL}}}{\text{TL}_i}. \quad (4)$$

Thus, the term $-\frac{\beta_{\text{TL}}}{\text{TL}_i}$ reduces the expected grid cell-level abundance λ_{it} by the sampling exposure rate, $\phi_i(\text{TL}_i)$, of the transect within the grid cell when estimating μ_{it} . The estimated value for β_{TL} determines the rate of sampling saturation as the transect length increases (which is determined in part by the average home range size and habitat use of each species), and eventually μ_{it} approaches λ_{it} as $\text{TL}_i \rightarrow \infty$. This formulation allowed us to make predictions at the grid cell level for λ_{it} and N_{it} by setting the term $-\frac{\beta_{\text{TL}}}{\text{TL}_i}$ equal to zero in Equation (4) (Kéry & Royle, 2015). Because the rate of sampling saturation is likely to vary between grid cells based on the distribution of habitat, roads, and bat home ranges in each, we modeled β_{TL_i} as a random slope by transect i (Appendix S2: Section S3). When $\phi_i(\text{TL}_i)$ is estimated near zero, it also functionally serves as an additional process to explain zeros in the observed data, making the consideration of a hurdle process from Doser et al. (2021) redundant. Finally, we dealt with missing transect lengths by estimating a transect length proxy for all routes in the NABat database, which was calculated as the shortest linear distance connecting all sampled point locations along each transect (including bat detections, NoID files, and noise files). Then, using a submodel

within our estimating model, we estimated the error distribution between the proxy length and true transect length where both occurred. The latter informed estimates of transect length given the proxy where values for the transect length were not provided (Appendix S2: Section S3).

Count observation model

We developed our observation model based on transect-level abundances (M_{it}), thus our notation differs from previous work that uses N_{it} to represent abundance. However, the observation model itself is equally applicable in systems without this additional thinning process (i.e., N_{it} could be swapped back for M_{it} throughout this section). Acoustic detectors were deployed via mobile transects at $i = 1, \dots, R$ grid cells for a total of $j = 1, \dots, J$ survey nights each time period (year and season), and repeated across time periods $t = 1, \dots, T$ (where time periods are indexed by year then season, e.g., $t = 1$ for the prevolancy season in year 1, $t = 2$ for the postvolancy season in year 1). For each grid cell i , visit j , and time period t , the observed response v_{ijt} was total counts of auto IDs to the target species of interest.

Similar to previous formulations of hypergeometric, false-positive, occupancy models (Chambert, Waddle, et al., 2018), Doser et al. (2021) used a hurdle approach to model ambiguous counts. Although potentially helpful in situations with zero inflation, the hurdle process is not required for model identifiability and can lead to convergence issues as abundance gets large (Doser et al., 2021). Furthermore, the hurdle specification results in two sets of false-positive rates and detection rates (one for the detection/nondetection data and one set for the nonzero count data), which complicates the interpretation of these parameters and any effects their covariates might have on the observation process. Thus, we specified an observation model without the hurdle process and instead used a single Poisson regression to model the auto IDs v_{ijt} as:

$$v_{ijt} \sim \text{Poisson}(M_{it} \times \delta_{ijt} + \omega_{ijt}). \quad (5)$$

In Equation (5), there are two rates of observation bias: δ_{ijt} , which is the average detection rate per individual, and ω_{ijt} , which is the average number of false-positive detections per survey based on an implicit source of false positives (i.e., without an explicit term for the presence or abundance of other species). In our application, the average detection rate per individual δ_{ijt} at each location i , night j , and time period t is a product of

the: (1) encounter rate of individual bats with the “cone-of-detection” of the mobile detector, (2) the echolocation rate, and (3) the probabilities of successfully recording and correctly classifying the echolocation sequence. The false-positive rate ω_{ijt} could vary by the type of acoustic monitoring hardware and software used or by differences in the abundance and activity of other bat species. Our formulation for the total count of auto IDs (v_{ijt}) in Equation (3) (before including heterogeneity on δ and ω) was identical to the auto ID count model described by Clement et al. (2022) for their single-species, false-positive N-mixture model. However, our modeling framework differed from Clement et al. (2022) in several important ways including: (1) we modeled heterogeneity in δ and ω in space and time, (2) we did not rely on parameter constraints ($\delta > \omega$) for identifiability, and (3) we used a hypergeometric observation model (Doser et al., 2021) to estimate observation rates and latent abundance states directly from a subset of manually reviewed data.

Manual review observation model

A subset of species auto IDs (v_{ijt}) was manually reviewed by NABat partners (Reichert et al., 2018) and the total that was reviewed n_{ijt} and confirmed k_{ijt} as the species of interest was recorded for each sampling night. Following Doser et al. (2021), we used a hypergeometric observation model for the manually reviewed data (e.g., Chambert, Waddle, et al., 2018; Kéry & Royle, 2020). The latent number of true-positive detections K_{ijt} came from a binomial distribution given the total count of species auto IDs (v_{ijt}) and the true-positive rate (p_{ijt}); where p_{ijt} was defined as a function of the transect-level abundance (M_{it}), the average detection rate (δ_{ijt}), and the false-positive rate (ω_{ijt}):

$$K_{ijt} \sim \text{Binomial}(p_{ijt}, v_{ijt}), \tag{6}$$

$$p_{ijt} = \frac{(M_{it} \times \delta_{ijt})}{(M_{it} \times \delta_{ijt} + \omega_{ijt})}. \tag{7}$$

The latent number of false positives was estimated as $Q_{ijt} = v_{ijt} - K_{ijt}$. The number of confirmed acoustic files k_{ijy} was modeled based on a hypergeometric function given K_{ijt} , Q_{ijt} , and n_{ijt} as:

$$k_{ijt} \sim \text{Hypergeometric}(K_{ijt}, Q_{ijt}, n_{ijt}). \tag{8}$$

Thus, this model supported instances where only a subset of files was manually reviewed within any given sampling night.

Application to modeling bat abundance from mobile transect acoustics

We made several modifications to the model that estimates bat abundance and population trends over time at landscape scales. Full details are documented in Appendix S2: Sections S1–S3.

Modeling heterogeneity in δ and ω

If models do not account for systemic heterogeneity in either average detection rates (δ) or false-positive rates (ω), trend estimates of occupancy and abundance will be biased (Clare et al., 2021; Miller et al., 2015; Wright et al., 2020). Rather than using a zero-truncated negative binomial sampling distribution to account for unmodeled heterogeneity in both δ and ω in the expected count (e.g., Doser et al., 2021), we modeled separate covariates and random effects distributions for each source of observation bias (δ_{ijt} and ω_{ijt}). In general, bat activity tends to be low at the start of the year in temperate parts of North America where the study species occur; it increases as temperatures warm, as female behavior changes postparturition (after birth), and as young become volant. It declines as temperatures cool, bats eventually move to their fall and winter ranges, and many species enter hibernation (Gorman et al., 2021). These life history considerations on bat activity are commonly modeled using day-of-year effects, which often explain a large portion of the temporal variance (e.g., Cole et al., 2022; Gorman et al., 2021; Whitby et al., 2014). To explain differences in detection by year, sampling night, and location, we included a random effect of year, in addition to linear and quadratic day-of-year effects with random slopes by location (Appendix S2: Section S1). To account for an increase in activity and abundance each year after young become volant, we estimated different abundances ($\lambda_{it}, N_{it}, \mu_{it}, M_{it}$) prevolancy and postvolancy and included a postvolancy covariate effect in Equations (1) and (4).

Next, we accounted for spatiotemporal heterogeneity in the false-positive rate using observation-level random effects (i.e., sampling night by transect) nested within NABat project random effects (Appendix S2: Section S2). These project random effects helped control for differences in detector types, classification software, and manual vetting protocols used among data contributors; the observation-level random effects helped account for heterogeneity in the false-positive rate due to high variability in sources of false positives (e.g., co-occurring bats, background noise, cluttered environments) between sampling nights and locations (e.g., Kéry & Royle, 2015).

Predictive covariates

We included a suite of abiotic and biotic predictors summarized at the NABat grid cell level to model abundance (Equation 1). These predictors were measures of climate (average annual temperature, average annual precipitation, WorldClim 2.0, Fick & Hijmans, 2017), landcover (proportion of forest cover of any kind, proportion of wetlands, NALC, 2010), building density (Microsoft, Bing Maps Team, 2019), elevation (Maximum elevation, USGS GTOPO30, USGS, 1999), physiographic diversity (Theobald et al., 2015), and seasonal migratory population connectivity (Appendix S2: Section S4.2, using data from Weins et al., 2023); see Appendix S2, and Appendix S2: Table S1 for more details on covariates. Based on previously hypothesized relationships between bat roosting and foraging preferences in areas of diverse habitats and topologies (e.g., Humphrey, 1975) (especially those with trees, insects, plants, water, rocky crevices, and talus slopes), we expected positive relationships for proportion forest cover, proportion wetlands cover, and physiographic diversity. Physiographic diversity is a measure of landscape complexity that considers multiple factors (multiscale topographic position, slope, aspect, parent material, continuous heat load) and is correlated with plant diversity (Theobald et al., 2015). Next, the importance of buildings as maternity colony habitat for big brown bats and little brown bats is also well known (e.g., Barbour & Davis, 1969); however, because urban areas may generally lack foraging habitat, we included linear and quadratic effects to allow the relationship between abundance and building density to saturate or even decline at very high building densities. We also modeled linear and quadratic effects of maximum elevation and average annual temperature given that extremes in both variables occur across North America, and the optimal range for many species may fall at intermediate values.

Linking winter and summer populations and quantifying WNS impacts

We included a winter-to-summer (i.e., migratory) connectivity metric as a spatiotemporal predictor of abundance for each grid cell and year. This connectivity metric linked summer and winter populations based on the seasonal migration behavior of each species. Specifically, they link the population abundance in known winter roosts (i.e., locations in the NABat database with “winter colony counts”) each year from a separate status and trends analysis (Wiens et al., 2023) with expected abundance in the summer distribution each year. We calculated a

“potential metapopulation connectivity metric” (Moilanen & Hanski, 2001) that predicted the relative number of migrants each summer to each grid cell based on: (1) the abundance of bats in the prior winter each year in each known hibernaculum, and (2) the probability that winter and summer locations were connected, which was calculated based on seasonal migration kernels for each species (with one parameter – average seasonal migration distance) and the distance between each documented hibernaculum and grid cell. In addition to serving as a potentially useful spatial predictor of bat summer populations, this approach also provided us a way of linking regional trends over time in winter populations with those in summer populations. For example, winter abundances for little brown bats and tricolored bats have declined drastically because the arrival of WNS, with regional differences depending on the timing of WNS arrival (Cheng et al., 2021). Thus, this metric captured the potential spatiotemporal influence of WNS impacts on known winter populations and the summer abundance distribution.

Using the approach described in Appendix S2: Section S4.2, we calculated the potential winter-to-summer connectivity for each grid cell each year using the weighted average of the seasonal migration distance for each species based on data reported in the literature (see Appendix S2: Tables S2 and S3 for more details). R code for deriving the winter-to-summer connectivity covariate for each species has been made publicly available on Gitlab as part of a USGS software release (Udell et al., 2024a). Because of the low availability of winter colony count data in the western USA and Canada, we only used these metrics as predictors of abundance in the eastern portion of the range for little brown bats and big brown bats. In contrast, winter-to-summer connectivity was used as a predictor throughout the modeled species range for tricolored bat (a predominantly eastern species).

Model specification and regularization for each species

Year was included as a time-varying intercept (i.e., factor effect) and was applied to species differently. For tricolored bats, a single time-varying intercept was included throughout the entire modeled range of the species. For little brown bats and big brown bats, a separate, time-varying intercept was included for each of two regions given observed differences in monitoring data sets and the progression of the cold-growing fungus that causes WNS (*Pseudogymnoascus destructans*, Pd): an East region with monitoring data dating back through 2012, where the

winter-to-summer population connectivity metric was relevant given the number of known hibernacula; and a Northwest region with monitoring data dating back through 2016, where the connectivity metric was not relevant due to limited information on the whereabouts of hibernacula. An autoregressive (AR1) process was also modeled on the time-varying intercept of each region to share information across years (Appendix S2: Section S5).

A base model with all covariates was initially considered for each species (except for building density, which was only included for little brown bats and big brown bats based on known regular use of buildings by each species). Separate covariate effects by region were also included for little brown bats to allow for potential differences in species behavior (e.g., Blejwas et al., 2023; Weller et al., 2018). Covariates were removed from the final model of each species based on model fit (i.e., posterior predictive checks) and uncertainty of covariate effects (e.g., large variances with credible intervals overlapping zero). We used Laplace priors for covariate effects on species abundance to provide model regularization, minimizing the effects of covariates that provided little information while also limiting the issues of moderate correlations among some predictors (Hooten & Hobbs, 2015). For these priors, we used a scale parameter of $\sqrt{2}$, which resulted in a variance of 1.

Model fitting and criticism

We fitted models in a Bayesian framework using JAGS (Plummer, 2003) and the *JagsUI* package (Kellner et al., 2019) in program R (R Core Team, 2020) (see Appendix S2: Section S6 for Markov Chain Monte Carlo [MCMC] settings). Models were assessed for convergence by visually assessing chains and using the r-hat statistic of Gelman and Rubin (1992) that indicates convergence when values are near 1. Model fit was assessed with posterior predictive checks on the counts of auto IDs each night v_{jit} by calculating the Bayesian p -values (values near zero or one indicate poor fit while 0.5 indicates a perfect fit) and c-hat (the overdispersion statistic, or “lack-of-fit ratio,” where a value of 1 suggests a perfect fit, and values much larger than 1 suggest poor fit and overdispersion) based on chi-squared residuals (Kéry & Royle, 2015). R code for formatting data, setting up and running each species’ model, making predictions, and calculating status and trends—in addition to simplified model vignettes—have been made publicly available on Gitlab as a USGS software release (Udell et al., 2024a).

Status and trends estimates at multiple scales

For the purposes of these analyses, we treated relative abundance estimates at each spatial scale (transect, grid cell, state/province, modeled species range) as the measure of population status, and changes in these estimates over time as a measure of trend. At the transect level, for each year we estimated the expected value μ_{it} and abundance state M_{it} ; at the grid cell level, we predicted the expected value λ_{it} of the abundance state N_{it} .

We made predictions for all grid cells in the modeled species range using 10,000 MCMC samples from the fitted model. Given that the prevolancy season is the primary season of interest for status and trends (Loeb et al., 2015), we only made predictions for the prevolancy season each year. Thus, for all prediction and trend calculations, the index t corresponds to year instead of “time period” (season and year). Because bats are highly mobile, these abundances correspond with the total (or in our application, relative) number of bat home ranges (i.e., the superpopulation abundance) intersecting each spatial extent. For inferences across larger spatial extents (e.g., states, range-wide), we calculated the average relative abundance $\hat{\lambda}_t$ each year across all grid cells in the region of interest as a derived parameter over all MCMC samples k , where λ_t^k denotes all samples for each $\hat{\lambda}_t$ as:

$$\hat{\lambda}_t^k = \frac{\sum_i \lambda_{it}^k}{N_{\text{cells}}} \tag{9}$$

We then summarized the posterior distributions by taking the means, medians, standard deviations, and 95% credible intervals (95% CRIs) for each region and year. Although the sum across relative abundances ($\sum_i \lambda_{it}$) can be calculated in given regions, we caution against using this sum as an absolute population estimate because (1) bats are mobile and home ranges of individual bats can occur across several grid cells and (2) if all assumptions of the modeling framework (e.g., saturation sampling) were not met, or if there were sampling biases (e.g., likely road bias), then we would be making inferences to relative abundance rather than absolute abundance (Barker et al., 2018; DiRenzo et al., 2019; Link et al., 2018). Furthermore, because we did not make predictions for the entire range of each species, status, and trend estimates correspond with the portion of the population that occurs in the modeled species range.

We derived three different measures of population trend over two different time periods (2017–2020 and 2012–2020), first as the ratio of population change $\left(\Delta_t = \frac{\hat{\lambda}_t}{\hat{\lambda}_{t-1}}\right)$ (i.e., population growth rate where values of

1 indicate no growth) for calculation purposes, then as the proportional rate of change (by subtracting 1 from the final values), which we report for a more natural interpretation (i.e., -0.10 indicates the population declined by 10%). To avoid confusion with the expected relative abundance estimate (λ_{it}), we denoted the annual change from year $t-1$ to year t as Δ_t , the geometric average as Δ_{Gavg} , and the total rate of change as Δ_{tot} . We calculated regional-level trends using $\hat{\lambda}_t$, and grid cell-level trends using λ_{it} . We derived samples of the posterior distribution for the geometric average as $\Delta_{Gavg}^k = \left(\prod_{t=2}^T \Delta_t^k \right)^{\frac{1}{T-1}}$, noting that it yields the same results as $\Delta_{Gavg}^k = \left(\Delta_{tot}^k \right)^{\frac{1}{T-1}}$ using Δ_{tot}^k as the total ratio of change $\left(\Delta_{tot}^k = \frac{\hat{\lambda}_t}{\lambda_{t=1}} \right)$ (before subtracting one). For each derived trend variable, we summarized their respective posterior distributions by calculating the means, medians, standard deviations, 95% credible intervals, and the probability that the trend parameter was negative. For tricolored bats, we did not provide trend estimates at the grid cell level for Florida and portions of Texas because of data limitations (sampled only in later years).

RESULTS

Species detections

We detected big brown bats most by auto ID (29,387), with an overall manual review rate of 0.162 (4787 files reviewed), and an overall confirmation rate of 0.583 (2793 files confirmed). Tricolored bats were detected a total of 23,517 times by auto ID, with an overall manual review rate of 0.195 (4576 files reviewed) and an overall confirmation rate of 0.615 (2813 files confirmed). Little brown bats were detected the least (9784 auto IDs), with an overall manual review rate of 0.603 (5902 files reviewed) and an overall confirmation rate of 0.196 (1157 files confirmed). Survey effort for each species is reported in Appendix S3: Figures S1–S3.

Final models for each species

The final model used for each species is reported in Table 1. The model for tricolored bats retained all predictors of abundance at the grid cell level. For big brown bats and little brown bats, maximum elevation was dropped due to high correlations with physiographic diversity (0.85) and uncertain estimated effects (i.e., overlapping zero) when it was included. All other

predictors were retained for big brown bats. For little brown bats, average annual temperature, average annual precipitation, and the proportion of wetlands were dropped as predictors in the Northwest region due to highly uncertain effects (large standard errors and credible intervals overlapping zero). The model fit for each species, as measured by Bayesian p -values and overdispersion statistics (c -hat), showed no evidence for lack-of-fit and we observed negligible overdispersion (i.e., c -hat values, were very close to one for all models, Table 1). Full tables of parameter estimates for each species model are available in Appendix S3: Tables S1–S3. Comprehensive population status and trends inferences for each species have also been provided at the transect, grid cell, state/province, and range-wide scales as a USGS data release (Udell et al., 2024b).

Sampling exposure and detection by species

Sampling exposure (e.g., the proportion of bats in a grid cell that may be encountered along a transect) is an increasing and saturating function of transect length, and this relationship was strongest for tricolored bats, followed by big brown bats and little brown bats (Figure 1A). The relationships between average detection rates and the day of the year for tricolored bats and little brown bats were positive and log-linear, and rates of detection were higher for tricolored bats than for little brown bats (Figure 1B). This relationship for big brown bats was best fit by a concave quadratic relationship peaking around the cut-off date of prevolancy (15 July, day 196), and was lower than the other species until approximately day 150 when the average detection rate of big brown bats equaled that of little brown bats, and by day 190 it was nearly the same as tricolored bats.

Relative abundance of tricolored bats

For tricolored bats, we found positive log-linear effects on abundance for winter-to-summer connectivity, physiographic diversity, wetlands, and forest cover; whereas we found a negative effect of average precipitation (Figure 2). The average temperature had a concave quadratic relationship (highest at intermediate values) with abundance but shifted strongly toward higher temperatures due to a strong positive effect on the linear term. Maximum elevation had the opposite pattern, with a negative linear term and a very weak positive quadratic term. The factor effects of year on relative abundance (with respect to the intercept in 2012) had increasingly negative point

TABLE 1 Model description for each species including the specification of the time-varying intercept, covariate predictors, and model fit statistics (Bayesian *p*-value and c-hat) of each.

Species	Intercept	Covariates			Bayesian	
		Range-wide	Both regions	East only	<i>p</i> -value	c-hat
Tricolored bat (<i>Perimyotis subflavus</i>)	Range-wide, time-varying intercept	Elevation, elevation ² , average annual temperature, average annual temperature ² , physiographic diversity, average annual precipitation, proportion forest cover, proportion wetlands cover, winter-to-summer connectivity			0.315	1.034
Little brown bat (<i>Myotis lucifugus</i>)	Time-varying intercept for each region (East and Northwest) with an autoregressive AR1 process		Proportion forest cover, physiographic diversity, building density, building density ²	Average annual temperature, average annual temperature ² , average annual precipitation, proportion wetlands cover, winter-to-summer connectivity	0.430	1.019
Big brown bat (<i>Eptesicus fuscus</i>)	Time-varying intercept for each region (East and Northwest) with an autoregressive AR1 process		Average annual temperature, average annual temperature ² , physiographic diversity, average annual precipitation, proportion forest cover, proportion wetlands cover, building density, building density ²	Winter-to-summer connectivity	0.359	1.018

estimates from 2013 to 2020, with probabilities greater than 0.9 for all years but 2014 (Appendix S3: Table S1). The random intercepts for the average detection rate each year (on the log scale) varied from -1.084 (-1.661 to -0.636) in 2020 to -0.309 (-0.580 to 0.067) in 2012. For additional parameter estimates for tricolored bats, see Appendix S3: Table S1.

Maps of the predicted relative abundance distribution at the 100 km² grid cell level for tricolored bats each year λ_{it} are depicted in Figure 3A (2012) and Figure 3B (2020). Predictions were made across the modeled range for each species (i.e., the geographic extent within the confines of the monitoring data). To aid visualization, a log transformation was used for the color scale, but the corresponding numbers in the legend are provided on a natural scale. The median point estimates for λ_{it} ranged from nearly zero to as high as 175 individuals, with the highest relative abundances in year 2012. The total rate of change in λ_{it} for each grid cell between 2012 and 2020 is depicted in Figure 3C, along with the WNS spread map

by county and year. Median estimates of tricolored bats ranged from around -0.50 (-50%) to -0.78 (-78%), with the strongest declines estimated in regions that have been impacted by WNS during the years of monitoring (2012–2020). The timeseries of the average grid cell-level relative abundance across the modeled species range each year $\hat{\lambda}_t$ is depicted in Figure 3D, which shows the marked decline in tricolored bats from 2012 to 2020. Across the modeled species range, the population declined a total of 61.5% (95% CRI: 21.7%–77.5%) at an annual rate of decline of 11.2% each year (95% CRI: 3.0%–17.0%, Table 2).

Relative abundance of little brown bats

We found positive effects of forest cover, winter-to-summer connectivity, wetlands, and physiographic diversity on the abundance of little brown bats in the East region, and a negative effect of precipitation (Figure 2). We also found

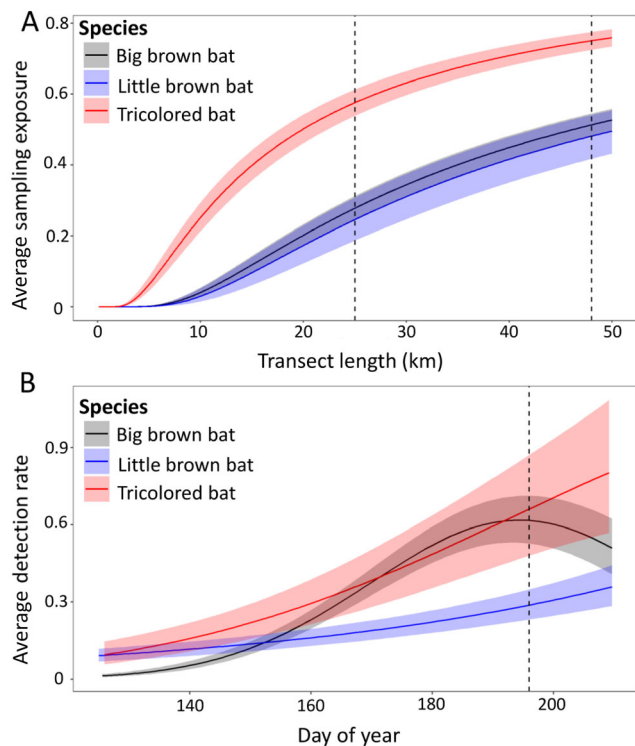


FIGURE 1 Estimated relationships of the average sampling exposure ϕ_i (i.e., using the mean of the random effects distribution) given mobile acoustic transect length, and the average detection rate per individual given day of year for each species. Species shown are big brown bat (*Eptesicus fuscus*), little brown bat (*Myotis lucifugus*), and tricolored bat (*Perimyotis subflavus*). (A) The estimated relationship between average sampling exposure and transect length for each species. The dashed vertical reference lines denote the recommended North American Bat Monitoring Program (NABat) transect length between 25 and 48 km. (B) Estimated relationship between detectability and day of year for each species. The dashed vertical line denotes 15 July, the threshold used to define prevolancy and postvolancy.

a positive effect with average temperature (the quadratic term was near zero). In the Northwest region, covariate effects trended in the same direction as the East region for physiographic diversity and forest cover, although the 95% credible intervals for these effects overlapped zero. In the Northwest region, the effect of building density was positive and log-linear, whereas the relationship in the East region was best fitted by a concave quadratic relationship with the highest expected abundance at intermediate values (Figures 2 and 4). The random intercept of year on expected relative abundance of little brown bats was mostly stable from 2012 to 2020 in the Northwest region but declined steadily from 2012 to 2020 in the East region (2012: mean = 1.707, 95% CRI = 1.320–2.072; 2020: mean = 1.301, 95% CRI = 0.899–1.668) (Appendix S3: Table S2). The random intercepts for the average detection rate each year

(on the log scale) varied from -1.518 (95% CRI = -1.761 to -1.237) in 2012 to -1.621 (95% CRI = -1.883 to -1.399) in 2013. For additional parameter estimates for little brown bats, see Appendix S3: Table S2.

Maps of the predicted relative abundance distribution at the 100 km^2 grid cell level for little brown bats each year λ_{it} are depicted in Figure 5A (2012) and Figure 5B (2020). The median point estimates for λ_{it} ranged from nearly zero to as high as 32 individuals, with the highest relative abundances in year 2012. The total rate of change in λ_{it} for each grid cell between 2012 and 2020 is depicted in Figure 5C along with the WNS spread map by county and year. Values for the grid cell-level estimates of the total rate of change from 2012 to 2020 ranged from around -0.029 (-0.3%) to -0.741 (-74%), with the strongest declines estimated in regions that have been impacted by WNS during the years of monitoring (2012–2020). The timeseries of the average grid cell-level relative abundance across the modeled range each year $\hat{\lambda}_t$ is depicted in Figure 5D, which shows the marked decline from 2012 to 2020. Across the modeled species range, the population declined a total of 38.6% (95% CRI: 16.2%–59.5%) at an annual rate of decline of 5.9% each year (95% CRI: 2.2%–10.7%, Table 2). In the East region, the population decline was 50.7% (95% CRI: 26.6%–68.2%) at an annual rate of decline of 8.5% each year (95% CRI: 3.8%–13.3%).

Relative abundance of big brown bats

For big brown bats, we found positive log-linear effects for forest cover, wetlands (across the modeled range), and winter-to-summer connectivity (East region only); and we found effects near zero of physiographic diversity and average precipitation (Figure 2). Average temperature had a concave quadratic relationship (highest at intermediate values) with abundance. The effect of buildings on the abundance of big brown bats was linear and positive with greater than a 95% certainty (Figures 2 and 3). The random intercept of year on expected relative abundance fluctuated over time in both regions and increased from 2012 to 2020 (Appendix S3: Table S3). Random intercepts for the average detection rate each year (on the log scale) varied from -0.815 (-1.046 to -0.646) in 2015 to -0.689 (-0.864 to -0.476) in 2012. For additional parameter estimates for big brown bats, see Appendix S3: Table S3.

Maps of the predicted relative abundance distribution at the 100 km^2 grid cell level for big brown bats each year λ_{it} are depicted in Figure 6A (2012) and Figure 6B (2020). The median point estimates for λ_{it} ranged from lows of nearly zero to highs near 52 individuals (in 2019). The total rate of change in λ_{it} for each grid cell between 2012

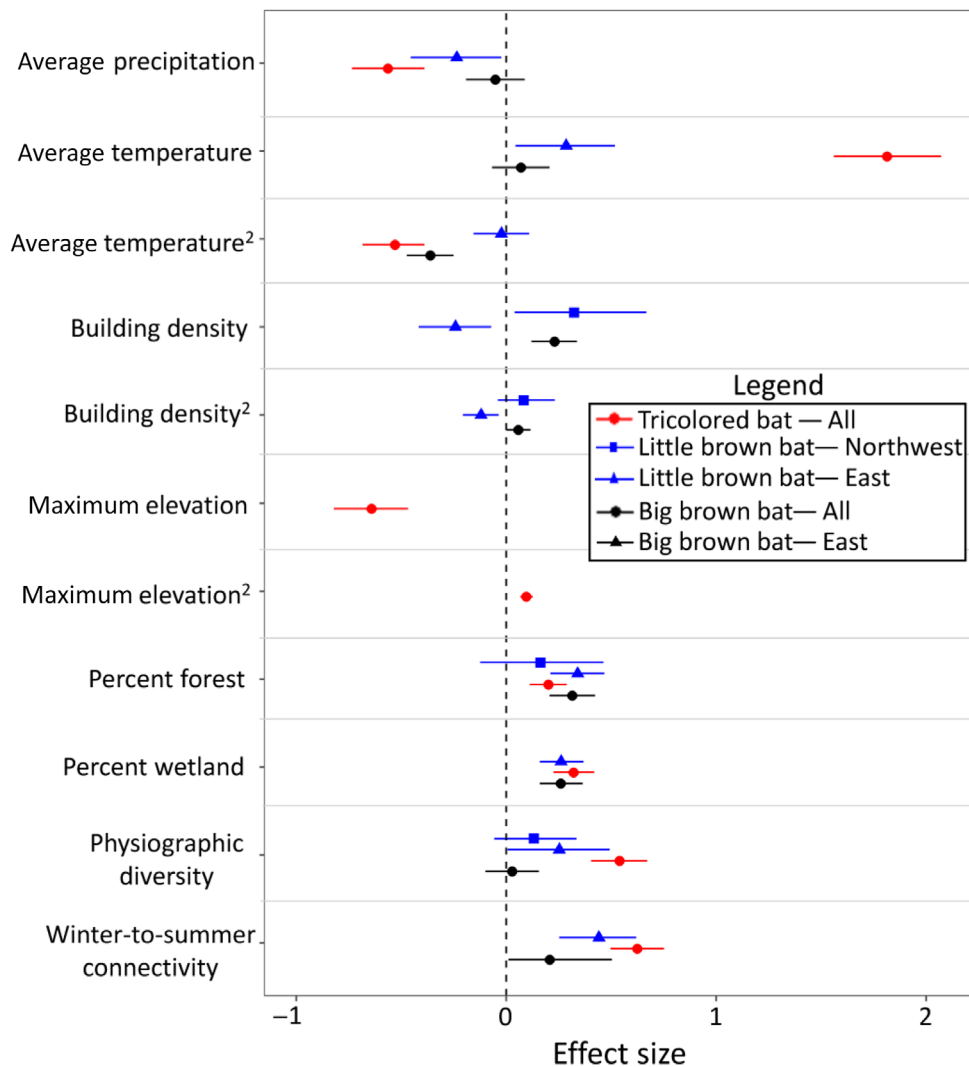


FIGURE 2 Grid cell-level covariate effects (means and 95% credible intervals) on the relative abundance of each species and region (where applicable). A reference line at zero denotes no effect. Species are big brown bat (*Eptesicus fuscus*), little brown bat (*Myotis lucifugus*), and tricolored bat (*Perimyotis subflavus*).

and 2020 is depicted in Figure 6C along with the WNS spread map by county and year. Values ranged from 0.24 (24%) to -0.13 (-13%) with a mix of increases and declines in regions impacted by WNS. The timeseries of the average relative abundance (at grid cell level) across the modeled species range each year $\hat{\lambda}_t$ is depicted in Figure 6D, which shows an increasing (11.5%) but uncertain ($Pr > 0 = 0.84$) population trend from 2012 to 2020.

DISCUSSION

We adapted recent formulations of false-positive N-mixture models to produce the first estimates of bat relative abundances in the summer maternity season from mobile transect acoustic monitoring and found major declines of two widespread bat species. Providing

information on population abundance and trends during this critical period for life history overcomes critical knowledge gaps in the ecology and conservation of North American bats. Our models advance the current paradigm of analyzing bat populations by explicitly incorporating imperfect detection, misclassification, and abundance processes in space and time. This modeling strategy isolates inference of population status and trends on the ecological variable of interest (abundance) and attempts to provide an unbiased means of estimating trends by accounting for spatiotemporal heterogeneities in each process. Failing to account for such systemic errors will bias trend estimates in space and time (e.g., Anderson, 2001; Clare et al., 2021; Miller et al., 2015; Wright et al., 2020). In addition to accounting for false-positive biases from misclassification error, as a “Poisson–Poisson N-mixture model”

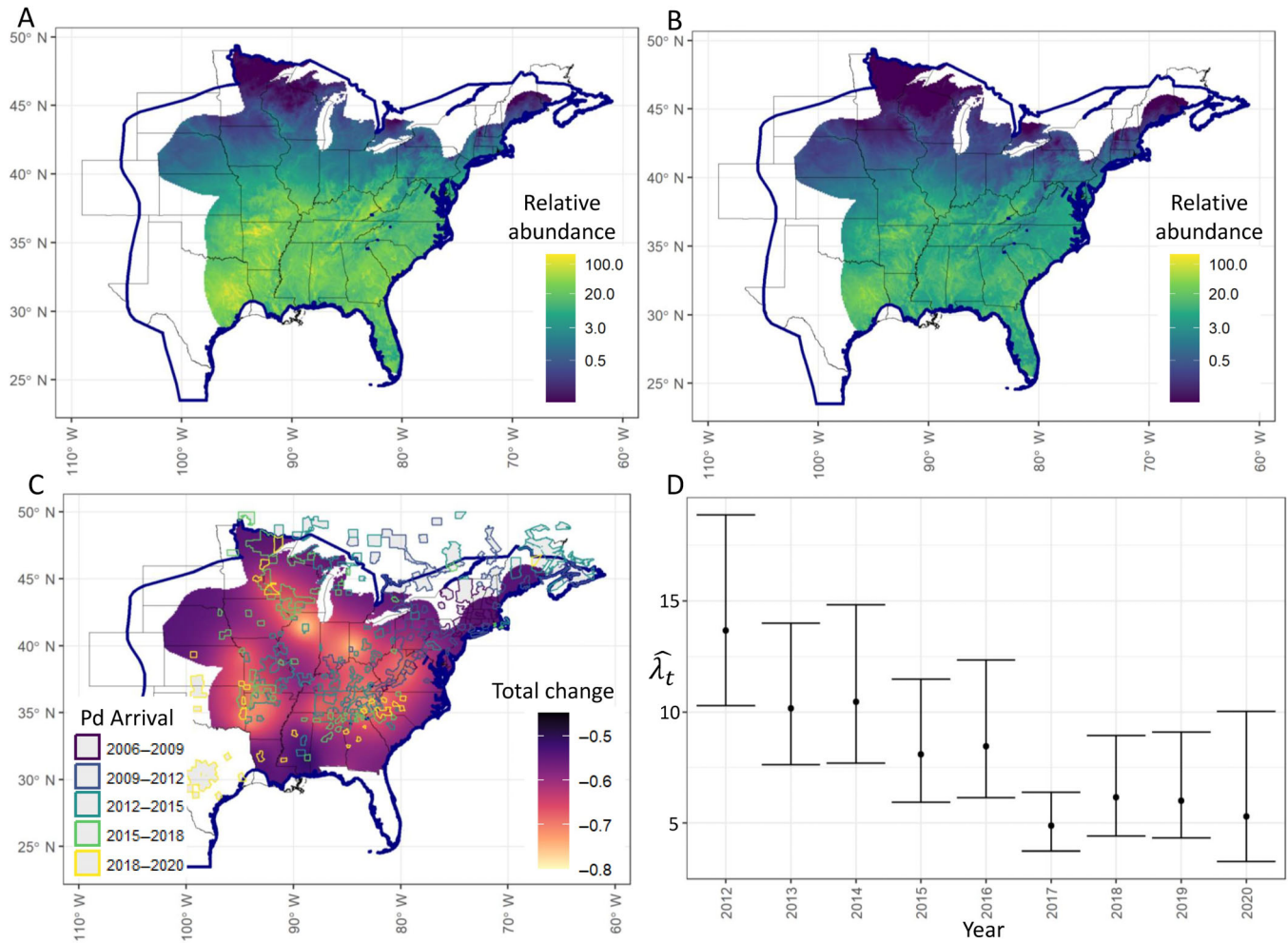


FIGURE 3 Relative abundance predictions for tricolored bats (*Perimyotis subflavus*) for each 100 km² grid cell in the modeled species range over time (2012 and 2020), the total change in grid cell abundances between 2012 and 2020, and the timeseries of the average relative abundance across the modeled species range. (A) Relative abundance predictions in each grid cell in 2012 (color bar on a log scale, relative abundance labels on natural scale). (B) Relative abundance predictions in each grid cell in 2020 (color bar on a log scale, relative abundance labels on natural scale). (C) Total proportional rate of change in the relative abundance of each grid cell between 2012 and 2020. Pd = the species name of the fungus that causes WNS, *Pseudogymnoascus destructans*. Pd year indicates the first year of Pd arrival (confirmed or suspected). (D) Timeseries of the average relative abundance across the modeled species range each year depicts the estimated declines from 2012 to 2020. Predictions are depicted against a reference range map (blue polygon; range from US Fish and Wildlife Service) and borders of US states (A–C) for illustrative purposes. Predictions are limited to the geographic scope of available monitoring data.

TABLE 2 Trends from 2012 to 2020 across the entire modeled range of each species. Species listed are big brown bat (*Eptesicus fuscus*), little brown bat (*Myotis lucifugus*), and tricolored bat (*Perimyotis subflavus*). Trend types include: Δ_{tot} , the total proportional rate of change from 2012 to 2020, and Δ_{Gavg} , the geometric average of the annual rate of change (displayed as proportional change) from 2012 to 2020. Standard deviation is denoted SD, the lower and upper bounds of the 95% credible intervals as LCI and UCI, respectively, and the probability that the trend is negative as $\text{Pr}(x < 0)$.

Species	Period	Trend type	Median	SD	LCI	UCI	$\text{Pr}(x < 0)$
Tricolored bat	2012–2020	Δ_{tot}	−0.615	0.142	−0.775	−0.217	0.996
Tricolored bat	2012–2020	Δ_{Gavg}	−0.112	0.035	−0.170	−0.030	0.996
Little brown bat	2012–2020	Δ_{tot}	−0.386	0.115	−0.595	−0.162	0.999
Little brown bat	2012–2020	Δ_{Gavg}	−0.059	0.023	−0.107	−0.022	0.999
Big brown bat	2012–2020	Δ_{tot}	0.115	0.130	−0.109	0.396	0.160
Big brown bat	2012–2020	Δ_{Gavg}	0.014	0.014	−0.014	0.043	0.160

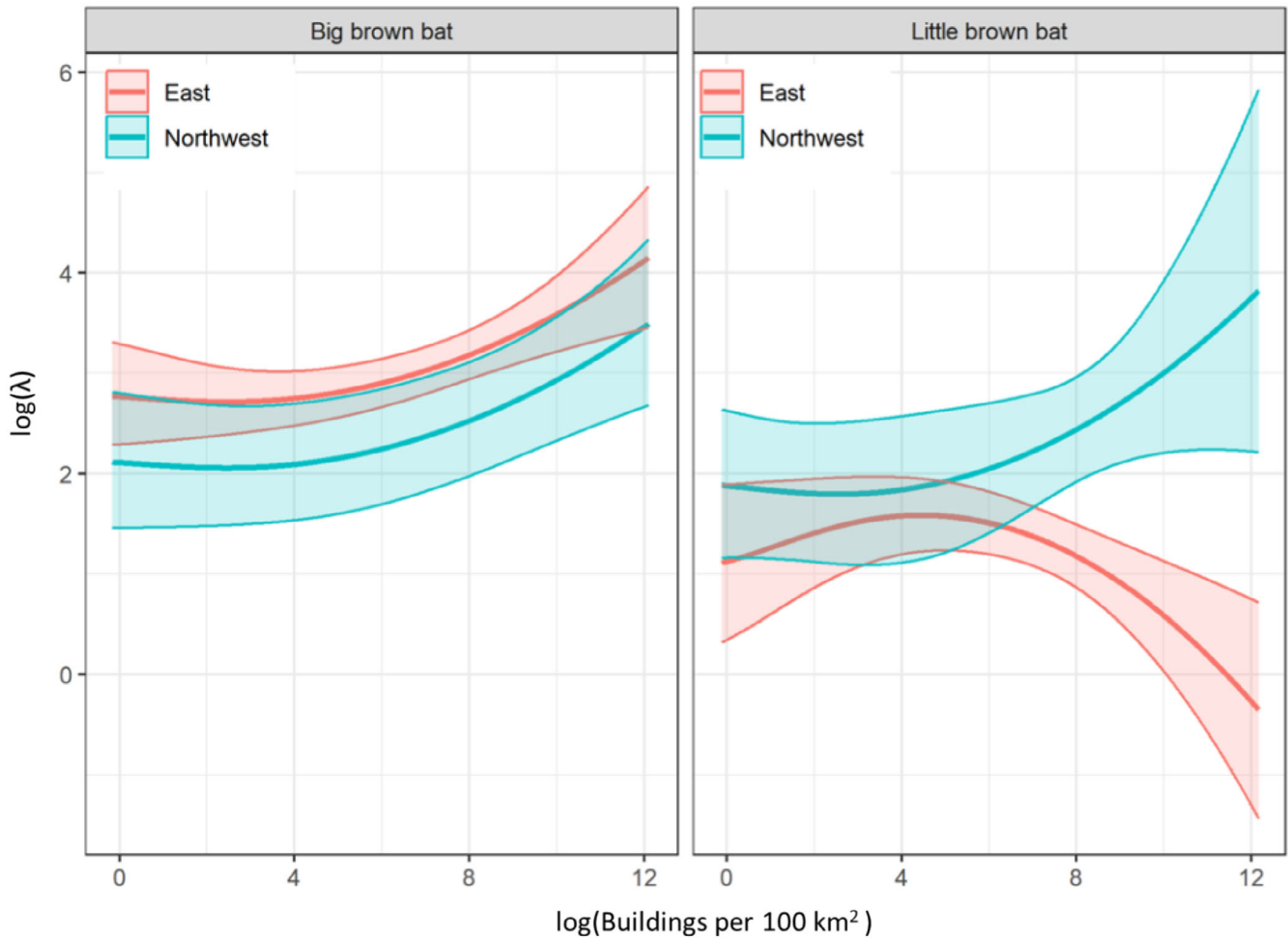


FIGURE 4 The estimated relationship between the log of building density and the log of expected relative abundance (λ) at the 100 km² grid cell level for little brown bats (*Myotis lucifugus*) and big brown bats (*Eptesicus fuscus*). A separate relationship was estimated for the East region and Northwest region for little brown bats, while a single relationship was estimated across both regions for big brown bats.

(Kéry & Royle, 2015; Nakashima, 2020; or more generally, an N-mixture model with a Poisson distribution for the observation process), our method is also robust to false-positive detections that arise from counting individuals more than once (Kéry & Royle, 2015; Nakashima, 2020). Therefore, this model could also estimate relative abundance from acoustic mobile transects conducted at slower speeds (e.g., transects conducted by bicycle, watercraft, or along winding mountain roads), or for faster flying species such as the Brazilian free-tailed bat (*Tadarida brasiliensis*). Our model might even produce useful relative abundance estimates from acoustic data gathered at stationary monitoring sites (e.g., Clement et al., 2022; Doser et al., 2021), yet more research is warranted to explore its efficacy in situations where average detection rates greatly exceed 1.0 (e.g., when individuals are typically encountered multiple times per visit at a stationary location), and detections can be highly clustered among individuals. Also, if integrated

with additional data sets that improve temporal coverage across the entire summer (i.e., prevolancy and postvolancy of young), our methods might provide a means for estimating bat reproductive rates (i.e., apparent birth rates) at macro scales for the first time.

We applied these newly developed models to determine the status and trends in summer abundance of three temperate North American bat species. Our approach allowed the first assessment of summertime bat relative abundance at multiple spatial scales (transect, grid cell, region, modeled species range). Using monitoring data collected and collated through the NABat monitoring program (including data collected under the NABat representative monitoring protocol), we provide a new analytical approach that allows (relative) abundance estimation and thus multiscale population inference ranging from local landscapes to entire continental ranges of bat species. We provide the first maps of relative abundance for these three species of bats that can inform

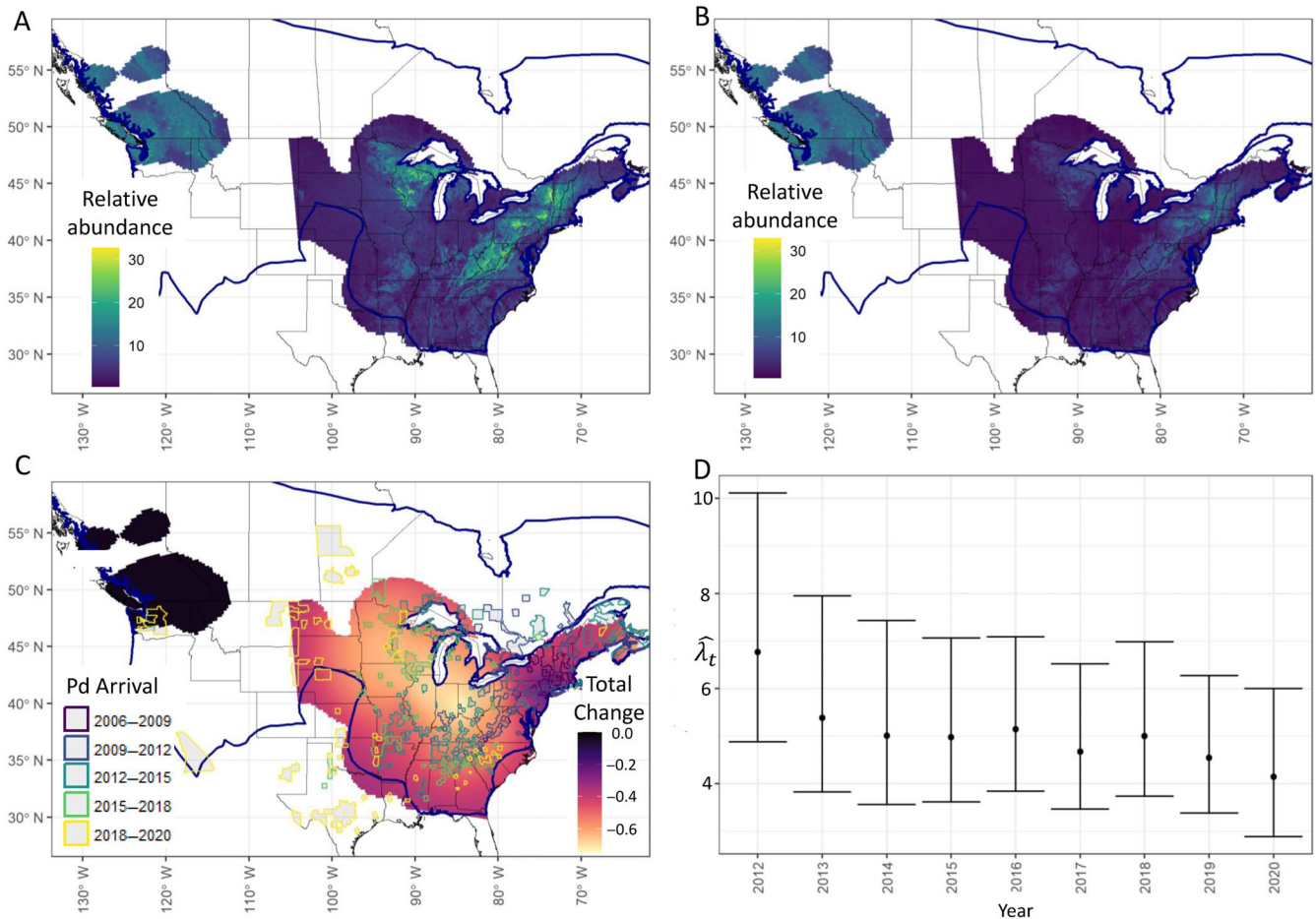


FIGURE 5 Relative abundance predictions for little brown bats (*Myotis lucifugus*) for each 100 km² grid cell in the modeled species range over time (2012 and 2020), the total change in grid cell abundances between 2012 and 2020, and the timeseries of the average relative abundance across the modeled species range. (A) Relative abundance predictions in each grid cell in 2012, on a natural scale. (B) Relative abundance predictions in each grid cell in 2020, on a natural scale. (C) Total proportional rate of change in the relative abundance of each grid cell between 2012 and 2020. Pd = the species name of the fungus that causes white-nose syndrome, *Pseudogymnoascus destructans*. Pd year indicates the first year of Pd arrival (confirmed or suspected). (D) Timeseries of the average relative abundance across the modeled species range each year depicts the estimated declines from 2012 to 2020. Predictions are depicted against a reference range map (blue polygon; National Atlas of the United States, 2011) and borders of US states (A–C) for illustrative purposes. Predictions are limited to the geographic scope of available monitoring data.

conservation management actions. Finally, using our winter-to-summer migratory connectivity approach, we linked spatiotemporal population changes in winter populations (reflecting primarily WNS impacts, in addition to natural interannual variation and any other unobserved population drivers) to spatiotemporal trends in relative abundance in the summer ranges of each species.

Overall trends in species relative abundances

From 2012 to 2020, we found strong evidence for precipitous declines (with probabilities >0.99) in the relative abundance of tricolored bats and little brown bats across

their modeled species ranges. The estimated total population decline was greater for tricolored bats than for little brown bats; however, our first year of monitoring began 6 years after the arrival of WNS in North America and after severe declines (>95% population losses) in the winter colonies of little brown bats in portions of the northeastern United States (e.g., Cheng et al., 2021; Turner et al., 2011; Wiens et al., 2023). Also, the estimated population decline for little brown bats in the East region was greater than that across the entire modeled species range. A separate analysis of mobile transect data from National Wildlife Refuges in the Southeast and Midwest United States (a subset of the data used here) over a similar timeframe (from 2012 to 2017) reported similar trends in activity for these species, where declines for

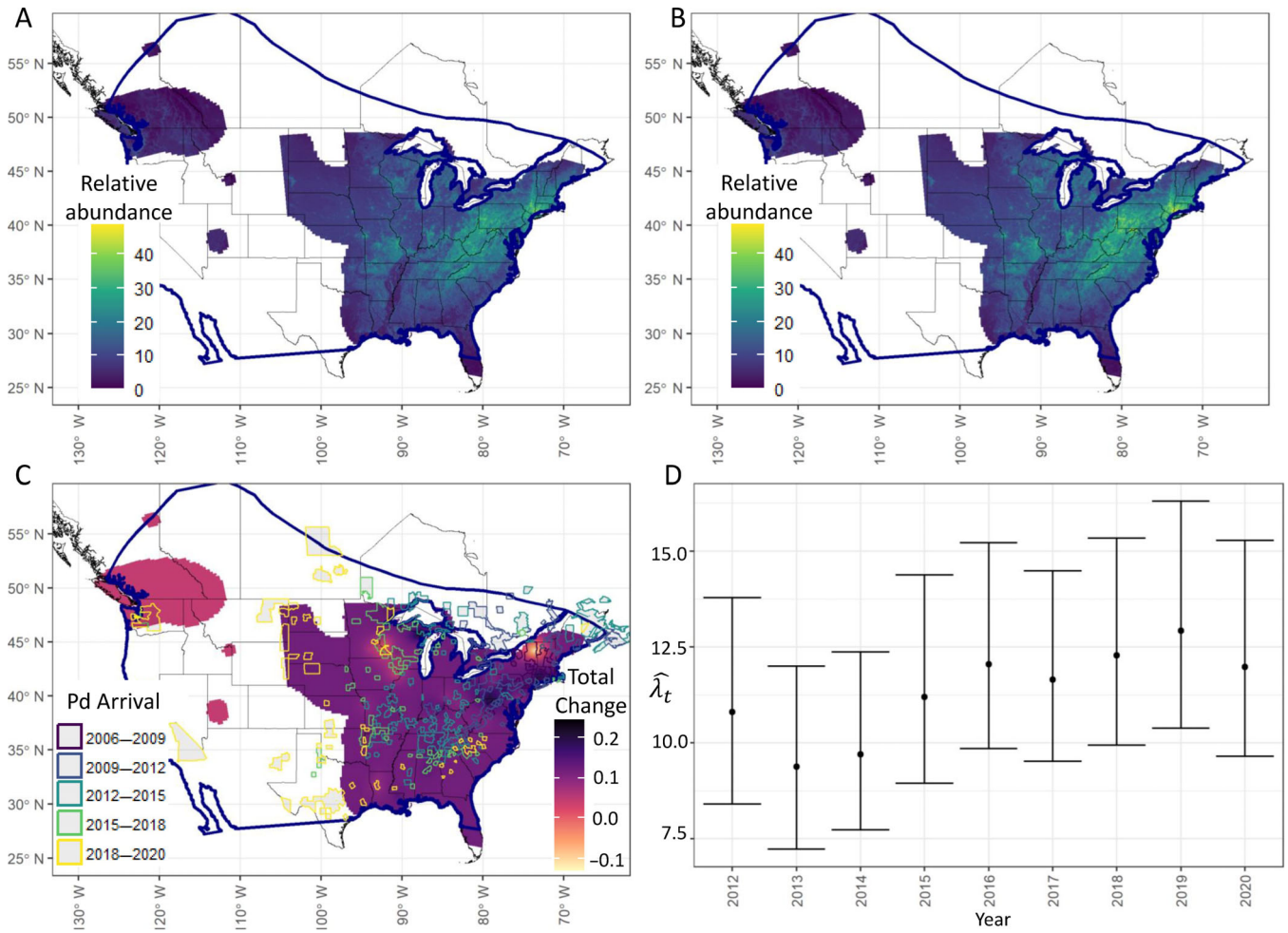


FIGURE 6 Relative abundance predictions for big brown bats (*Eptesicus fuscus*) for each 100 km² grid cell in the modeled species range in 2012 and 2020, the total change in relative abundance between 2012 and 2020, and the timeseries of the average relative abundance across the modeled species range. (A) Relative abundance predictions in each grid cell in 2012, on a natural scale. (B) Relative abundance predictions in each grid cell in 2020, on a natural scale. (C) Total proportional rate of change in the relative abundance of each grid cell between 2012 and 2020. Pd = the species name of the fungus that causes WNS, *Pseudogymnoascus destructans*. Pd year indicates the first year of Pd arrival (confirmed or suspected). (D) Timeseries of the average relative abundance across the modeled species range each year from 2012 to 2020. Predictions are depicted against a reference range map (blue polygon; National Atlas of the United States, 2011) and borders of US states (A–C) for illustrative purposes. Predictions are limited to the geographic scope of available monitoring data.

tricolored bats were larger than for little brown bats (Evans et al., 2021). Our work found that the estimated declines in relative abundance for tricolored bats and little brown bats were also larger than the estimated declines in occupancy probabilities from another recent analysis (Udell et al., 2022). These results are consistent with those from simulation studies (e.g., Ellis et al., 2014) that indicate that trends occupancy might be less sensitive to population declines when counts are greater than one because of the information reduction as a binary representation (e.g., Steen et al., 2023).

In contrast with inferred declines in populations of tricolored and little brown bats, annual trends in relative abundance for big brown bats over the same period showed a mix of regional increases and decreases across

the modeled species range (Figure 6), as well as a somewhat uncertain increase when aggregated across the entire modeled species range (Table 2). Previous work on big brown bat populations revealed a mix of decreases (e.g., Simonis et al., 2020) and increases (Pettit & O’Keefe, 2017) in detection rates because the emergence of WNS, which may be driven by a combination of minor WNS population impacts for big brown bats paired with larger WNS impacts to competitor species such as little brown bats and tricolored bats (i.e., competitive release, Jachowski et al., 2014; Johnson et al., 2021). From 2017 to 2020, the estimated trend for big brown bats in the Northwest region was near zero without strong support for an increase or decrease, which is consistent with a recent analysis of mobile transect data from British

Columbia (Rae et al., 2022). Less evidence for consistent population declines in big brown bats compared with the other species included in our analysis reflects observations over the past decade that this species seems less susceptible to the ravaging effects of the fungus that causes WNS than other hibernating bats in North America (Cheng et al., 2021).

Our approach for calculating trends over time differs from previous analyses of mobile transect data for bats. Prior efforts typically modeled trends while limiting spatial inference to the monitored transects (e.g., Britzke & Herzog, 2009; Roche et al., 2011) rather than expanding it to encompass larger landscapes. Although our new approach allowed spatial inference at the monitored transect scale (by estimating abundance M_{it} for each transect and time period), we were able to scale inference to much larger landscapes by integrating data from NABat's collective monitoring program with Bayesian hierarchical models. Not only did this upscaling allow us to infer population status and trends across spatially definable regions of interest, but it extended our ability to infer relative abundance in unsampled places.

Additional correlates of species abundance

We found that the abundance of all three bat species included in this study was positively influenced by the proportion of forest cover and wetlands. These associations were expected because bat roosts and foraging grounds are often associated with forested areas or are close to open water (O'Shea, Neubaum, et al., 2011). Previously, Evans et al. (2021) found that the proportion of woody cover near roads positively influenced the acoustic activity of little brown bats and big brown bats along mobile transects, but the woody cover was not an important predictor of tricolored bat activity in that study. Different results for tricolored bats in the latter study could be attributable to the smaller landscape context in which their analysis modeled forest cover, further indicating that our multiscale approach that quantified abundance predictors in a larger spatial context (i.e., at the 10 km × 10 km grid cell level) provides additional insight into bat populations.

The importance of habitat diversity and topographic diversity, given their relationship with the availability of roosting sites, has long been discussed in the literature as an important driver of bat distributions (e.g., Humphrey, 1975). We hypothesized a positive relationship between bat abundance and physiographic diversity because it was a measure of landscape complexity and potential niche diversity that is based on several factors (multiscale topographic position, aspect, slope, latitude,

parent material, and continuous heat index) and is positively correlated with plant diversity (Theobald et al., 2015). Indeed, we found a positive association between physiographic diversity and the abundance of tricolored bats and little brown bats, but no effect for big brown bats (Figure 2). Perhaps, not surprisingly, big brown bats may be among the most opportunistic of the species studied in terms of their ability to flourish by exploiting many different types of roost structures, both natural and human-made (Barbour & Davis, 1969).

We found building density had a positive log-linear relationship with the abundance of big brown bats across their entire modeled species range and for little brown bats in the Northwest region (Figure 4). Building density had a different effect on the modeled abundance of little brown bats in the East region, where the relationship was quadratic, suggesting the highest abundance at intermediate building densities and the lowest abundance at very high densities (Figure 4). In summer, both big brown bats and little brown bats are known to roost in human structures across a gradient of building densities from very rural areas (wildlands with few human structures) to urban areas (Barbour & Davis, 1969; Coleman & Barclay, 2011; Frick et al., 2009; Johnson et al., 2019; Neubaum et al., 2006; Tessler & Snively, 2014). While both species can be found in cities, big brown bats are especially common in urban areas during Nearctic summers (Neubaum et al., 2006; O'Shea, Ellison, & Stanley, 2011). For little brown bats, buildings are especially important as maternity roosts in regions without natural roosting habitat; for example, in prairies (Coleman & Barclay, 2011), or in regions with shorter summers and colder temperatures that pose energetic challenges to reproduction, such as at high elevations (e.g., Cryan et al., 2000; Johnson et al., 2019; Micalizzi et al., 2023) or higher latitudes such as Alaska (e.g., Tessler & Snively, 2014). Thus, buildings may provide suitable habitat for reproduction and allow for larger populations than would otherwise be supported (Johnson et al., 2019) and may even have allowed for range expansion into areas with otherwise unsuitable habitat (e.g., prairies and colder climates) as the number of buildings increased in North America (Kunz & Reynolds, 2003; Tessler & Snively, 2014).

Differences in the effects of building density on the abundance of little brown bats between the Northwest (consistent increase with building density) and East regions (increase at middle density and decrease at higher density) might be explained by generally higher latitudes and elevations (Johnson et al., 2019) found across the Northwest. Another plausible explanation for lower densities of little brown bats in urbanized areas of the East is that the species is competitively excluded

from building roosts by big brown bats that often exploit urban habitats (Whitaker & Gummer, 2000). In higher density urban centers, water bodies might be less accessible to foraging little brown bats or perhaps foraging opportunities in urban areas are compromised by lights, traffic, and/or other human disturbances. A study in Alberta, Canada (Coleman & Barclay, 2011) found that, while the abundance of little brown bats was higher in urban areas than in rural or urban-to-rural transition areas, body condition and individual fitness were highest in the urban-to-rural transition areas, which was attributed in part to intraspecific competition and lack of foraging habitat in urban areas. Our models indicated that average annual temperature influenced the abundance of all three species investigated, with the strongest positive effect for tricolored bats, and weaker positive effects for little brown bats and big brown bats. This conforms to theoretical expectations for small mammals and for smaller bats with high surface-area-to-volume ratios on tight energy budgets (Henshaw, 1970; Speakman & Thomas, 2003). We speculate that little brown bats and big brown bats may buffer themselves from the effects of outside temperature by roosting in buildings, perhaps explaining the weaker effects of average temperature than we observed with tricolored bats, which roost in buildings far less regularly (Barbour & Davis, 1969). Further research into the influence of urbanization on bat abundance using methods developed in this study could help explain why certain bat species are able to exploit human development and the presence, and thus potentially cope with population stressors, more than others.

Linking spatiotemporal trends in abundance of winter and summer populations

White-nose syndrome primarily infects and kills bats during hibernation while they are at their winter roosts or soon after they emerge from hibernation (Hoyt et al., 2021; Langwig et al., 2015). However, these impacts affect year-round spatiotemporal distributions of populations, likely including locations where Pd has not been detected. Inspired by metapopulation connectivity theory (e.g., Moilanen & Hanski, 2001), we calculated a winter-summer migratory connectivity metric that serves as a proxy for the relative number of bats migrating each year to each NABat grid cell given the spatial configuration of winter and summer habitats, species abundances at all known winter hibernacula, and average seasonal migration distance of each species. Our metric reflects biologically based hypotheses (seasonal life cycle and

migration behavior of each species) linking WNS-related population impacts in the winter range of each species with abundance in their summer range. Winter-to-summer connectivity based on available monitoring data played an important role in allowing us to quantitatively link bat populations across their winter and summer ranges. Given the strength of estimated covariate effects for winter-to-summer connectivity (Figure 2), modeling these seasonal population connections undoubtedly improved our ability to estimate spatiotemporal trends for each species, as well as let us predict regional declines (or in the case of big brown bats some regional increases) associated with WNS spread (Figures 2, 5, and 6).

A major limitation to modeling the effects of seasonally biased impacts like winter WNS mortality on bat populations, particularly when relying on summer survey data, is our inconsistent and incomplete understanding of bat hibernation habitat across North America. We modeled the winter distributions of each species based only on known hibernacula documented in the NABat database. Although coverage was good for these species in eastern and midwestern portions of North America, most hibernacula in western areas of the continent have not been found and described, probably because of inaccessibility, inconspicuousness, dispersion, and structural variability (Weller et al., 2018). Thus, low values for winter-to-summer connectivity for little brown bats and big brown bats observed in northwestern North America likely reflect data limitations rather than biologically low population connectivity (Appendix S2: Section S4.2). Furthermore, given the logistic difficulties of studying bat migration (e.g., weight limits of GPS tags, challenges in relocating migrating individuals in radio-tag studies), migration reports in the literature are rare, and band recoveries make up most of the verifiable reports (e.g., Cryan & Diehl, 2009). Given that some band recoveries may only reflect snapshots in a longer distance movement process, it is possible that some may underestimate the true migration distance. Future work could investigate how larger assumed migration distances influence estimates of relative abundance and trends. Additional discussion of modeling considerations, limitations, and future directions are provided in Appendix S2: Section S4.2.

Detection and sampling exposure (nonrandom availability)

In general, we found that average detection and sampling exposure rates were highest for tricolored bats, followed by big brown bats and little brown bats (Figure 1). Differences in sampling exposure between species were

likely to have been influenced by the distribution of habitat within a grid cell relative to roads, the distribution of bat roosts within a grid cell, movement distances of individual bats, and habitat selection of bats within their summer home ranges. Because these factors likely vary between grid cells and transects, we included a random effect distribution for the inverse transect length on sampling exposure for each species and transect to avoid potential biases. The higher average sampling exposure of tricolored bats could have been caused by larger movements of individuals and/or a higher likelihood of roosting or foraging in habitats near, over, or under roads (e.g., roosts in culverts). In this study and others (e.g., Whitby et al., 2014), tricolored bats and big brown bats were detected at much higher rates than species of *Myotis*, and possibly due to road bias (e.g., Braun de Torrez et al., 2017). Distribution of bat foraging and roosting habitat relative to roads within a grid cell is nonrandom and, unlike tricolored bats, the activity of little brown bats and big brown bats can be strongly tied to the amount of woody vegetation adjacent to roads (e.g., Evans et al., 2021).

We were able to scale population inference of abundance from the transect to the grid cell through saturation sampling (e.g., Royle et al., 2007). If road sampling bias was pervasive due to species avoidance of habitat near roads, abundance at the grid cell level would likely be underestimated. Our highest estimates of grid cell abundance for little brown bats (~32 bats) were much lower than the maximum number of bats reported in summer roosts; for example, before the arrival of WNS, maternity colonies were often hundreds to thousands of individuals (Anthony et al., 1981), or at higher latitudes in the tens to hundreds of individuals (Tessler & Snively, 2014). We were therefore likely to underestimate the absolute abundance of little brown bats due to road bias. The low confirmation rates of reviewed auto IDs for little brown bats could have also contributed to underestimating abundance, for which lack of confirmation due to uncertainty (e.g., downgrading a species detection to more general groupings such as *Myotis*) was currently treated as false positives.

Limitations and future work

Our estimates of abundance are best interpreted as relative abundance, rather than absolute abundance, at least until our models can be integrated with additional sources of monitoring data or their assumptions (such as saturation sampling) can be verified through field studies or informed via ancillary information. This is a conservative approach, because in general when assumptions of

N-mixture models are violated, inference shifts from absolute abundance to relative abundance (DiRenzo et al., 2019; Link et al., 2018). Extending our models to include habitat covariates for transects (e.g., kernel methods from Evans et al., 2021; fine-scale point pattern process approximations from Kéry & Royle, 2020) in addition to the habitat covariates of grid cells that we modeled, may help to correct for any availability biases and provide additional information to inform the multiscale abundance process. Formal integration of our abundance estimation methods with monitoring data that were not gathered along roads (e.g., stationary acoustics, captures, or roost counts) could also help to vet our model assumptions and overcome some of these limitations. For example, the inclusion of capture/recapture data could help to overcome the limitations of unmarked abundance methods in general (e.g., Link et al., 2018), the inclusion of stationary acoustic data could help to overcome road bias and improve geographic coverage, and the inclusion of summer roost counts could “ground truth” the otherwise relative estimates of abundance in sampled grid cells.

We used data from a manual review process based on confirmation/rejection of auto IDs (Reichert et al., 2018) to estimate false-positive rates by assuming they were true; however, manual review is prone to human limitations including the possibility of being wrong, potential differences in acceptance probabilities between observers and, in the case of little brown bats and other species of *Myotis*, the tendency to downgrade auto IDs when uncertain. Regardless, manually reviewing data remained the best approach for estimating false-positive rates given our data sets, especially considering the alternatives. For example, for tricolored bats our posterior estimates for detection rates (δ_{ijt}) were only greater than the expected number of false positives (ω_{ijt}) for ~82% of observations, meaning that a significant proportion of our estimates would be biased on the parameter constraints of Clement et al. (2022) (i.e., that $\delta > \omega$). Future work may seek to overcome these limitations by including software confusion matrices as informed priors (e.g., Stratton et al., 2022) or by using classification probability scores (rather than discrete values; e.g., Kéry & Royle, 2020).

Despite the robust representative sampling protocol for NABat, clear geographic biases exist in data from mobile acoustic transects across the ranges of some species that restricted population inferences from the entire range to the “modeled species range.” For example, much of western North America remains unsampled due to challenges accessing many areas by road, or where sinuous mountain roads require slower speeds for safety reasons. Such roads were initially discouraged for mobile transects to minimize the chances of double-counting

individuals (Loeb et al., 2015). However, recent work suggests that mobile transects may be more appropriate in these regions than previously assumed (Rojas et al., 2022) and conducting more mobile transects in such regions would rectify geographic biases and could allow for more comprehensive inference across the range of each species. Furthermore, as a Poisson–Poisson N-mixture model, our methods can reliably estimate abundance even when animals are detected more than once (e.g., Nakashima, 2020), addressing concerns when ideal speeds (i.e., less than 32 km/h) cannot be accommodated by available roads.

CONCLUSION

We estimated the first status and trends in the summer abundance of bat populations across large portions of their ranges using new formulations of unmarked abundance methods and acoustic recordings of bats along driving transects. For the first time, acoustic data gathered by mobile transect protocols and collated through the NABat program were used to monitor bat populations across spatial scales ranging from local landscapes to large portions of species ranges. Patterns detected by this research are more ecologically informative than those based on less direct proxies of abundance (e.g., occupancy, activity) and are likely to be more robust than patterns based on statistical methods that do not attempt to control for biases from detection and misclassification processes that vary in space and time. Using this approach, we found precipitous declines in two widespread bat species linked to WNS. Our approach is applicable to many species of bats in North America that can be monitored using acoustic detectors or are amenable to other monitoring systems in which biases from imperfect detection and misclassification processes are common. Indeed, modest false-positive rates are likely to be common across many wildlife monitoring programs that use visual or auditory point counts (e.g., McClintock et al., 2010; Miller et al., 2015). Finally, by providing a means to estimate abundance using a point pattern process model, the expected abundance predicted by our mobile acoustic transect model can serve as a scaffolding for a single, integrated status and trends model that also links relative abundance estimates with bat occupancy from stationary acoustic data and capture data (e.g., Miller et al., 2019).

AUTHOR CONTRIBUTIONS

All authors contributed to project conceptualization, critical review, and writing the manuscript. Bradley J. Udell led the analysis and the initial draft of the manuscript. Bradley J. Udell, Brian E. Reichert, Kathryn M. Irvine,

and Wayne E. Thogmartin contributed to developing the analytical methods used in this analysis.

ACKNOWLEDGMENTS

We thank all NABat partners and members of the NABat Core Planning Team for their contributions, without which this work would not be possible. Next, we thank Jeffery Doser, Adam Smith, Eric Britzke, and Michael Whitby for early discussions about the methods we applied in this work. Any use of trade, firm, or product names is for descriptive purposes only and does not imply endorsement by the US Government. The findings and conclusions in this article are those of the authors and do not necessarily represent the views of the US Fish and Wildlife Service.

CONFLICT OF INTEREST STATEMENT

The authors declare no conflicts of interest.

DATA AVAILABILITY STATEMENT

Some of the data supporting this research are sensitive and only available from the North American Bat Monitoring Program (NABat) database with restrictions, and the parameters of the dataset drawn from the NABat database for this analysis, including the date of the export and database version, are documented within this paper and are also available on the NABat Data Request Archive in NABat Request Number 34 and NABat Request Number 108 at <https://sciencebase.usgs.gov/nabat/#/data/requests/all>. Requests to access the sensitive data can be made by following the steps documented at <https://www.nabatmonitoring.org/get-data>. All non-sensitive data, model outputs, and predictions (Udell et al., 2024b) are publicly available in the USGS ScienceBase repository at <https://doi.org/10.5066/P9WYSBBN>. Code (Udell et al., 2024a) is publicly available in the USGS Gitlab repository at <https://doi.org/10.5066/P9R3W0EZ>.

ORCID

Bradley J. Udell  <https://orcid.org/0000-0001-5225-4959>

Kathryn M. Irvine  <https://orcid.org/0000-0002-6426-940X>

Jeremy T. H. Coleman  <https://orcid.org/0000-0002-2762-947X>

Brian E. Reichert  <https://orcid.org/0000-0002-9640-0695>

REFERENCES

- Anderson, D. R. 2001. "The Need to Get the Basics Right in Wildlife Field Studies." *Wildlife Society Bulletin* 29: 1294–97.
- Anthony, E. L. P., M. H. Stack, and T. H. Kunz. 1981. "Night Roosting and the Nocturnal Time Budget of the Little Brown Bat,

- Myotis lucifugus*: Effects of Reproductive Status, Prey Density, and Environmental Conditions.” *Oecologia* 51: 151–56.
- Banner, K. M., K. M. Irvine, T. J. Rodhouse, W. J. Wright, R. M. Rodriguez, and A. R. Litt. 2018. “Improving Geographically Extensive Acoustic Survey Designs for Modeling Species Occurrence with Imperfect Detection and Misidentification.” *Ecology and Evolution* 8: 6144–56.
- Barbour, R. W., and W. H. Davis. 1969. *Bats of America* 312. Lexington, KY: University Press of Kentucky.
- Barker, R. J., M. R. Schofield, W. A. Link, and J. R. Sauer. 2018. “On the Reliability of N-Mixture Models for Count Data.” *Biometrics* 74: 369–377.
- Blejwas, K., L. Beard, J. Buchanan, C. Lausen, D. Neubaum, A. Tobin, and T. J. Weller. 2023. “Could White-Nose Syndrome Manifest Differently in *Myotis lucifugus* in Western Versus Eastern Regions of North America? A Review of Factors.” *Journal of Wildlife Diseases* 59: 381–397.
- Bötsch, Y., L. Jenni, and M. Kéry. 2020. “Field Evaluation of Abundance Estimates under Binomial and Multinomial N-Mixture Models.” *Ibis* 162(3): 902–910.
- Braun de Torrez, E. C. B., M. A. Wallrichs, H. K. Ober, and R. A. McCleery. 2017. “Mobile Acoustic Transects Miss Rare Bat Species: Implications of Survey Method and Spatio-Temporal Sampling for Monitoring Bats.” *PeerJ* 5: e3940.
- Britzke, E. R., and C. Herzog. 2009. *Using Acoustic Surveys to Monitor Population Trends in Bats*. Vicksburg, MS: US Army Engineer Research and Development Center.
- Chambert, T., E. H. C. Grant, D. A. Miller, J. D. Nichols, K. P. Mulder, and A. B. Brand. 2018. “Two-Species Occupancy Modelling Accounting for Species Misidentification and Non-detection.” *Methods in Ecology and Evolution* 9: 1468–77.
- Chambert, T., D. A. W. Miller, and J. D. Nichols. 2015. “Modeling False Positive Detections in Species Occurrence Data under Different Study Designs.” *Ecology* 96: 332–39. <https://doi.org/10.1890/14-1507.1>.
- Chambert, T., J. H. Waddle, D. A. Miller, S. C. Walls, and J. D. Nichols. 2018. “A New Framework for Analysing Automated Acoustic Species Detection Data: Occupancy Estimation and Optimization of Recordings Post-Processing.” *Methods in Ecology and Evolution* 9: 560–570.
- Cheng, T. L., J. D. Reichard, J. T. H. Coleman, T. J. Weller, W. E. Thogmartin, B. E. Reichert, A. B. Bennett, et al. 2021. “The Scope and Severity of White-Nose Syndrome on Hibernating Bats in North America.” *Conservation Biology* 35: 1586–97.
- Clare, J. D., P. A. Townsend, and B. Zuckerberg. 2021. “Generalized Model-Based Solutions to False-Positive Error in Species Detection/Nondetection Data.” *Ecology* 102(2): e03241.
- Clement, M. J., J. A. Royle, and R. J. Mixan. 2022. “Estimating Occupancy from Autonomous Recording Unit Data in the Presence of Misclassifications and Detection Heterogeneity.” *Methods in Ecology and Evolution* 13(8): 1719–29. <https://doi.org/10.1111/2041-210X.13895>.
- Cole, H. J., D. G. Gomes, and J. R. Barber. 2022. “EcoCountHelper: An R Package and Analytical Pipeline for the Analysis of Ecological Count Data Using GLMMs, and a Case Study of Bats in Grand Teton National Park.” *PeerJ* 10: e14509.
- Coleman, J. L., and R. M. Barclay. 2011. “Influence of Urbanization on Demography of Little Brown Bats (*Myotis lucifugus*) in the Prairies of North America.” *PLoS One* 6(5): e20483.
- Costa, A., A. Romano, and S. Salvadio. 2020. “Reliability of Multinomial N-Mixture Models for Estimating Abundance of Small Terrestrial Vertebrates.” *Biodiversity and Conservation* 29: 2951–65.
- Cryan, P. M., M. A. Bogan, and J. S. Altenbach. 2000. “Effect of Elevation on the Distribution of Female Bats in the Black Hills, South Dakota.” *Journal of Mammalogy* 81(3): 719–725.
- Cryan, P. M., and R. H. Diehl. 2009. “Analyzing Bat Migration.” In *Ecological and Behavioral Methods for the Study of Bats*, edited by T. H. Kunz and S. Parsons, 476–488. Baltimore, MD: Johns Hopkins University Press.
- D’Acunto, L. E., B. P. Pauli, M. Moy, K. Johnson, J. Abu-Omar, and P. A. Zollner. 2018. “Timing and Technique Impact the Effectiveness of Road-Based, Mobile Acoustic Surveys of Bats.” *Ecology and Evolution* 8(6): 3152–60.
- DiRenzo, G. V., C. Che-Castaldo, S. P. Saunders, E. H. C. Grant, and E. F. Zipkin. 2019. “Disease-Structured N-Mixture Models: A Practical Guide to Model Disease Dynamics Using Count Data.” *Ecology and Evolution* 9(2): 899–909.
- Doser, J. W., A. O. Finley, A. S. Weed, and E. F. Zipkin. 2021. “Integrating Automated Acoustic Vocalization Data and Point Count Surveys for Estimation of Bird Abundance.” *Methods in Ecology and Evolution* 12(6): 1040–49.
- Ellis, M. M., J. S. Ivan, and M. K. Schwartz. 2014. “Spatially Explicit Power Analyses for Occupancy-Based Monitoring of Wolverine in the US Rocky Mountains.” *Conservation Biology* 28(1): 52–62.
- Environment and Climate Change Canada. 2018. *Recovery Strategy for the Little Brown Myotis (Myotis lucifugus), the Northern Myotis (Myotis septentrionalis), and the Tri-Colored Bat (Perimyotis subflavus) in Canada. Species at Risk Act Recovery Strategy Series* 172. Ottawa: Environment and Climate Change Canada.
- Evans, K. O., A. D. Smith, and D. Richardson. 2021. “Statistical Power of Mobile Acoustic Monitoring to Detect Population Change in Southeastern US Bat Species, a Case Study.” *Ecological Indicators* 125: 107524.
- Farr, M. T., T. O’Brien, C. B. Yackulic, and E. F. Zipkin. 2022. “Quantifying the Conservation Status and Abundance Trends of Wildlife Communities with Detection–Nondetection Data.” *Conservation Biology* 36(6): e13934.
- Ficetola, G. F., B. Barzaghi, A. Melotto, M. Muraro, E. Lunghi, C. Canedoli, E. Lo Parrino, et al. 2018. “N-Mixture Models Reliably Estimate the Abundance of Small Vertebrates.” *Scientific Reports* 8(1): 10357.
- Fick, S. E., and R. J. Hijmans. 2017. “Worldclim 2: New 1-Km Spatial Resolution Climate Surfaces for Global Land Areas.” *International Journal of Climatology* <http://www.worldclim.com/version> 37: 4302–15.
- Fletcher, R. J., Jr., T. J. Hefley, E. P. Robertson, B. Zuckerberg, R. A. McCleery, and R. M. Dorazio. 2019. “A Practical Guide for Combining Data to Model Species Distributions.” *Ecology* 100(6): e02710.
- Frick, W. F., T. Kingston, and J. Flanders. 2020. “A Review of the Major Threats and Challenges to Global Bat Conservation.” *Annals of the New York Academy of Sciences* 1469: 5–25. <https://doi.org/10.1111/nyas.14045>.
- Frick, W. F., D. S. Reynolds, and T. H. Kunz. 2009. “Influence of Climate and Reproductive Timing on Demography of Little Brown Myotis *Myotis lucifugus*.” *Journal of Animal Ecology* 79: 128–136.

- Friedenberg, N. A., and W. F. Frick. 2021. "Assessing Fatality Minimization for Hoary Bats amid Continued Wind Energy Development." *Biological Conservation* 262: 109309. <https://doi.org/10.1016/j.biocon.2021.109309>.
- Gelman, A., and D. B. Rubin. 1992. "Inference from Iterative Simulation Using Multiple Sequences." *Statistical Science* 7(4): 457–511.
- Gorman, K. M., E. L. Barr, L. Ries, T. Nocera, and W. M. Ford. 2021. "Bat Activity Patterns Relative to Temporal and Weather Effects in a Temperate Coastal Environment." *Global Ecology and Conservation* 30: e01769.
- Hayes, J. P., H. K. Ober, and R. E. Sherwin. 2009. "Survey and Monitoring of Bats." In *Ecological and Behavioral Method for the Study of Bats*, 2d ed., edited by T. H. Kunz and S. Parsons, 112–129. Baltimore, MD: Johns Hopkins University Press.
- Hayward, B., and R. Davis. 1964. "Flight Speeds in Western Bats." *Journal of Mammalogy* 45: 236–242.
- Henshaw, R. E. 1970. "Thermoregulation in Bats." *SMU Scholar, Fondren Science Series* 1(11): 188–232.
- Hooten, M. B., and N. T. Hobbs. 2015. "A Guide to Bayesian Model Selection for Ecologists." *Ecological Monographs* 85(1): 3–28.
- Hoyt, J. R., A. M. Kilpatrick, and K. E. Langwig. 2021. "Ecology and Impacts of White-Nose Syndrome on Bats." *Nature Reviews Microbiology* 19(3): 196–210.
- Humphrey, S. R. 1975. "Nursery Roosts and Community Diversity of Nearctic Bats." *Journal of Mammalogy* 56(2): 321–346.
- Jachowski, D. S., C. A. Dobony, L. S. Coleman, W. M. Ford, E. R. Britzke, and J. L. Rodrigue. 2014. "Disease and Community Structure: White-Nose Syndrome Alters Spatial and Temporal Niche Partitioning in Sympatric Bat Species." *Diversity and Distributions* 20(9): 1002–15.
- Johnson, C., D. J. Brown, C. Sanders, and C. W. Stihler. 2021. "Long-Term Changes in Occurrence, Relative Abundance, and Reproductive Fitness of Bat Species in Relation to Arrival of White-Nose Syndrome in West Virginia, USA." *Ecology and Evolution* 11(18): 12453–67.
- Johnson, J. S., J. J. Treanor, A. C. Slusher, and M. J. Lacki. 2019. "Buildings Provide Vital Habitat for Little Brown Myotis (*Myotis lucifugus*) in a High-Elevation Landscape." *Ecosphere* 10: e02925.
- Kellner, K., M. Meredith, and M. K. Kellner. 2019. "Package 'jagsUI'." CRAN Repos.
- Kéry, M., and J. A. Royle. 2015. *Applied Hierarchical Modeling in Ecology: Analysis of Distribution, Abundance and Species Richness in R and BUGS* 783. Amsterdam: Academic Press Inc.
- Kéry, M., and J. A. Royle. 2020. *Applied Hierarchical Modeling in Ecology: Analysis of Distribution, Abundance and Species Richness in R and BUGS: Volume 2: Dynamic and Advanced Models* 787. Amsterdam: Academic Press Inc.
- Kunz, T. H., and D. S. Reynolds. 2003. "Bat Colonies in Buildings." In *Monitoring Trends in Bat Populations of the United States and Territories: Problems and Prospects*. Reston, VA: U.S. Geological Survey, Biological Resources Division, Information and Technology Report, USGS/BRD/ITR–2003-0003, edited by T. J. O'Shea and M. A. Bogan, 91–102.
- Langwig, K. E., W. F. Frick, R. Reynolds, K. L. Parise, K. P. Drees, J. R. Hoyt, T. L. Cheng, T. H. Kunz, J. T. Foster, and A. M. Kilpatrick. 2015. "Host and Pathogen Ecology Drive the Seasonal Dynamics of a Fungal Disease, White-Nose Syndrome." *Proceedings of the Royal Society B: Biological Sciences* 282(1799): 20142335.
- Loeb, S. C., T. J. Rodhouse, L. E. Ellison, C. L. Lausen, J. D. Reichard, K. M. Irvine, T. E. Ingersoll, et al. 2015. *A Plan for the North American Bat Monitoring Program (NABat)* 1–112. Asheville, NC: United States Department of Agriculture, Forest Service, Research and Development, Southern Research Station.
- Link, W. A., M. R. Schofield, R. J. Barker, and J. R. Sauer. 2018. "On the Robustness of N-Mixture Models." *Ecology* 99(7): 1547–51.
- Martin, J., D. Smith, H. Li, M. Hall, E. Ferrall, J. Rae, B. Straw, and B. Reichert. 2022a. *North American Bat Monitoring Program (NABat) Mobile Acoustic Transect Surveys Standard Operating Procedure 1—Locating and Establishing Mobile Transect Routes*. Reston, VA: USGS Publications Warehouse. <https://doi.org/10.3133/tm2C1>.
- Martin, J., D. Smith, H. Li, M. Hall, E. Ferrall, J. Rae, B. Straw, and B. Reichert. 2022b. *North American Bat Monitoring Program (NABat) Mobile Acoustic Transect Surveys Standard Operating Procedure 2—Field Season and Survey Preparation*. Reston, VA: USGS Publications Warehouse. <https://doi.org/10.3133/tm2C2>.
- Martin, J., D. Smith, H. Li, M. Hall, E. Ferrall, J. Rae, B. Straw, and B. Reichert. 2022c. *North American Bat Monitoring Program (NABat) Mobile Acoustic Transect Surveys Standard Operating Procedure 3—Conducting Mobile Transect Surveys*. Reston, VA: USGS Publications Warehouse. <https://doi.org/10.3133/tm2C3>.
- McClintock, B. T., L. L. Bailey, K. H. Pollock, and T. R. Simons. 2010. "Experimental Investigation of Observation Error in Anuran Call Surveys." *The Journal of Wildlife Management* 74(8): 1882–93.
- Micalizzi, E. W., S. A. Forshner, E. B. Low, B. Johnston, S. A. Skarsgard, and R. M. R. Barclay. 2023. "Female Little Brown Bats Require Both Building and Natural Roosts in a Mountainous Environment with Short Summers." *Ecosphere* 14(12): e4731.
- Microsoft, Bing Maps Team. 2019. "Computer Generated Building Footprints for the United States and Canada." <https://github.com/Microsoft/USBuildingFootprints>.
- Miller, D. A., L. L. Bailey, E. H. C. Grant, B. T. McClintock, L. A. Weir, and T. R. Simons. 2015. "Performance of Species Occurrence Estimators When Basic Assumptions Are Not Met: A Test Using Field Data Where True Occupancy Status Is Known." *Methods in Ecology and Evolution* 6(5): 557–565.
- Miller, D. A., J. D. Nichols, B. T. McClintock, E. H. Campbell, L. L. Bailey, and L. A. Weir. 2011. "Improving Occupancy Estimation when Two Types of Observational Error Occur: Non-detection and Species Misidentification." *Ecology* 92(7): 1422–28.
- Miller, D. A., K. Pacifici, J. S. Sanderlin, and B. J. Reich. 2019. "The Recent Past and Promising Future for Data Integration Methods to Estimate Species' Distributions." *Methods in Ecology and Evolution* 10(1): 22–37.
- Moilanen, A., and I. Hanski. 2001. "On the Use of Connectivity Measures in Spatial Ecology." *Oikos* 95(1): 147–151.
- Nakashima, Y. 2020. "Potentiality and Limitations of N-Mixture and Royle-Nichols Models to Estimate Animal Abundance Based on Noninstantaneous Point Surveys." *Population Ecology* 62(1): 151–57.

- North American Bat Monitoring Program (NABat) Database v7.0.2 (Provisional Release): U.S. Geological Survey. 2021. Accessed 2021-10-18. NABat Request Number 34. <https://doi.org/10.5066/P9UXA6CF>
- North American Bat Monitoring Program (NABat) Database v7.0.20 (Provisional Release): U.S. Geological Survey. 2022. Accessed 2022-09-02. NABat Request Number 108. <https://doi.org/10.5066/P9UXA6CF>
- NALC. 2010. *2010 North American Land Cover at 250 m Spatial Resolution*. Produced by Natural Resources Canada/Canada Centre for Remote Sensing (NRCan/CCRS), United States Geological Survey (USGS), Insituto Nacional de Estadística y Geografía (INEGI), Comisión Nacional para el Conocimiento y Uso de la Biodiversidad (CONABIO) and Comisión Nacional Forestal (CONAFOR). Montréal, Québec, Canada: Commission for Environmental Cooperation. <http://www.cec.org/north-american-environmental-atlas/land-cover-2010-modis-250m/>.
- National Atlas of the United States. 2011. *North American Bat Ranges, 1830–2008*. Reston, VA: National Atlas of the United States <http://purl.stanford.edu/pz329xp4277>.
- Neubaum, D. J., T. J. O'Shea, and K. R. Wilson. 2006. "Autumn Migration and Selection of Rock Crevices as Hibernacula by Big Brown Bats in Colorado." *Journal of Mammalogy* 87(3): 470–79.
- O'Shea, T. J., and M. A. Bogan, eds. 2003. "Monitoring Trends in Bat Populations of the United States and Territories: Problems and Prospects." United States Geological Survey, Biological Resources Discipline, Information and Technology Report, USGS/BRD/ITR-2003-0003:1–274.
- O'Shea, T. J., P. M. Cryan, D. T. Hayman, R. K. Plowright, and D. G. Streicker. 2016. "Multiple Mortality Events in Bats." *Mammal Review* 46: 175–190. <https://doi.org/10.1111/mam.12064>.
- O'Shea, T. J., L. E. Ellison, and T. R. Stanley. 2004. "Survival Estimation in Bats: Historical Overview, Critical Appraisal, and Suggestions for New Approaches." In *Sampling Rare or Elusive Species: Concepts, Designs, and Techniques for Estimating Population Parameters*, edited by W. L. Thompson, 297–336. Washington, DC: Island Press.
- O'Shea, T. J., L. E. Ellison, and T. R. Stanley. 2011. "Adult Survival and Population Growth Rate in Colorado Big Brown Bats (*Eptesicus fuscus*)." *Journal of Mammalogy* 92: 433–443.
- O'Shea, T. J., D. J. Neubaum, M. A. Neubaum, P. M. Cryan, L. E. Ellison, T. R. Stanley, C. E. Rupprecht, W. J. Pape, and R. A. Bowen. 2011. "Bat Ecology and Public Health Surveillance for Rabies in an Urbanizing Region of Colorado." *Urban Ecosystems* 14: 665–697.
- Patterson, A. P., and J. W. Hadin. 1969. "Flight Speeds of Five Species of Vespertilionid Bats." *Journal of Mammalogy* 50: 152–53.
- Pettit, J. L., and J. M. O'Keefe. 2017. "Impacts of White-Nose Syndrome Observed during Long-Term Monitoring of a Midwestern Bat Community." *Journal of Fish and Wildlife Management* 8(1): 69–78.
- Plummer, M. 2003. "JAGS: A Program for Analysis of Bayesian Graphical Models Using Gibbs Sampling." In *Proceedings of the 3rd International Workshop on Distributed Statistical Computing (DSC 2003), Vienna, 20-22 March 2003*, Vol. 124 (125.10), 1–10.
- R Core Team. 2020. *R: A Language and Environment for Statistical Computing*. Vienna, Austria: R Foundation for Statistical Computing.
- Rae, J., C. Lausen, and B. Paterson. 2022. *North American Bat Monitoring Program in British Columbia: 2021 Data Summary and Activity Trend Analyses (2016–2021)* 1–105. Toronto: Wildlife Conservation Society, Canada and North American Bat Monitoring Program. <https://doi.org/10.19121/2022.Report.45336>.
- Reichert, B. E., M. Bayless, T. L. Cheng, J. T. H. Coleman, C. M. Francis, W. F. Frick, B. S. Gotthold, et al. 2021. "NABat: A Top-Down, Bottom-Up Solution to Collaborative Continental-Scale Monitoring." *Ambio* 50(4): 901–913.
- Reichert, B., C. Lausen, S. Loeb, T. Weller, R. Allen, E. Britzke, T. Hohoff, et al. 2018. "A Guide to Processing Bat Acoustic Data for the North American Bat Monitoring Program (NABat)." U.S. Geological Survey Open-File Report 2018, 33 p. <https://doi.org/10.3133/ofr20181068>.
- Roche, N., C. Catto, S. Langton, T. Aughney, and J. Russ. 2005. *Development of a car-based bat monitoring protocol for the republic of Ireland*. Irish Wildlife Manuals, No 19. Dublin (Ireland): National Parks and Wildlife Service, Department of Environment, Heritage and Local Government.
- Roche, N., S. Langton, T. Aughney, J. M. Russ, F. Marnell, D. Lynn, and C. Catto. 2011. "A Car-Based Monitoring Method Reveals New Information on Bat Populations and Distributions in Ireland." *Animal Conservation* 14(6): 642–651.
- Rojas, V. G., S. C. Loeb, and J. M. O'Keefe. 2022. "Applying Mobile Acoustic Surveys to Model Bat Habitat Use across Sinuous Routes." *Wildlife Society Bulletin* 46: e1353.
- Royle, J. A. 2004. "N-Mixture Models for Estimating Population Size from Spatially Replicated Counts." *Biometrics* 60(1): 108–115.
- Royle, J. A., M. Kéry, R. Gautier, and H. Schmid. 2007. "Hierarchical Spatial Models of Abundance and Occurrence from Imperfect Survey Data." *Ecological Monographs* 77(3): 465–481.
- Royle, J. A., and W. A. Link. 2006. "Generalized Site Occupancy Models Allowing for False Positive and False Negative Errors." *Ecology* 87(4): 835–841.
- Sherwin, H. A., W. I. Montgomery, and M. G. Lundy. 2013. "Bats and Climate Change." *Mammal Review* 43: 171–182. <https://doi.org/10.1111/j.1365-2907.2012.00214.x>.
- Simonis, M. C., B. K. Brown, and V. Bahn. 2020. "Mobile Bat Acoustic Routes Indicate Cavity-Roosting Species Undergo Compensatory Changes in Community Composition Following White-Nose Syndrome." *Acta Chiropterologica* 22(2): 315–326.
- Speakman, J. R., and D. W. Thomas. 2003. "Physiological Ecology and Energetics of Bats." In *Bat Ecology*, edited by T. H. Kunz and M. B. Fenton, 430–490. Chicago, IL: University of Chicago Press.
- Steen, V. A., A. Duarte, and J. T. Peterson. 2023. "An Evaluation of Multistate Occupancy Models for Estimating Relative Abundance and Population Trends." *Ecological Modelling* 478: 110303.
- Stevens, D. L., Jr., and A. R. Olsen. 2004. "Spatially Balanced Sampling of Natural Resources." *Journal of the American Statistical Association* 99(465): 262–278.

- Stratton, C., K. M. Irvine, K. M. Banner, W. J. Wright, C. Lausen, and J. Rae. 2022. "Coupling Validation Effort with In Situ Bioacoustic Data Improves Estimating Relative Activity and Occupancy for Multiple Species with Cross-Species Misclassifications." *Methods in Ecology and Evolution* 13(6): 1288–1303.
- Straw, B. R., J. A. Martin, J. D. Reichard, and B. E. Reichert, eds. 2022. "Analytical Assessments in Support of the U.S. Fish and Wildlife Service 3-Bat Species Status Assessment." Cooperator Report Prepared in Cooperation with the U.S. Geological Survey, United States Fish and Wildlife Service, and Bat Conservation International 271. <https://doi.org/10.7944/P9B4RWEU>.
- Talbert, C., and B. Reichert. 2018. "North American Grid-Based Sampling Frame: Continental United States." U.S. Geological Survey Data Release. <https://doi.org/10.5066/P9M00P17>.
- Tessler, D. F., and M. L. Snively. 2014. "New Insights on the Distribution, Ecology, and Overwintering Behavior of the Little Brown Myotis (*Myotis lucifugus*) in Alaska." *Northwestern Naturalist* 95(3): 251–263.
- Theobald, D. M., D. Harrison-Atlas, W. B. Monahan, and C. M. Albano. 2015. "Ecologically-Relevant Maps of Landforms and Physiographic Diversity for Climate Adaptation Planning." *PLoS One* 10(12): e0143619.
- Turner, G. G., D. Reeder, and J. T. Coleman. 2011. "A Five-Year Assessment of Mortality and Geographic Spread of White-Nose Syndrome in North American Bats, with a Look at the Future. Update of White-Nose Syndrome in Bats." *Bat Research News* 52: 13.
- U.S. Fish and Wildlife Service. 2022. *National Listing Workplan for Fiscal Years 2022–2027*. Washington, DC: U.S. Fish and Wildlife Service <https://www.fws.gov/media/national-listing-workplan-fiscal-years-2022-2027>.
- U.S. Fish and Wildlife Service. 2022a. "50 CFR Part 17. Endangered and Threatened Wildlife and Plants; Endangered Species Status for Northern Long-Eared Bat." *Federal Register* 87: 73488–504 <https://www.federalregister.gov/documents/2022/11/30/2022-25998/endangered-and-threatened-wildlife-and-plants-endangered-species-status-for-northern-long-eared-bat>.
- U.S. Fish and Wildlife Service. 2022b. "50 CFR Part 17. Endangered and Threatened Wildlife and Plants; Endangered Species Status for Tricolored Bat." *Federal Register* 87: 56381–83 <https://www.federalregister.gov/documents/2022/09/14/2022-18852/endangered-and-threatened-wildlife-and-plants-endangered-species-status-for-tricolored-bat>.
- U.S. Geological Survey. 1999. "GTOPO30." <https://doi.org/10.5066/F7DF6PQS>.
- Udell, B. J., B. Straw, T. L. Cheng, K. Enns, W. F. Frick, B. Gotthold, K. Irvine, et al. 2022. *Status and Trends of North American Bats: Summer Occupancy Analysis 2010–2019*. Fort Collins, CO: U.S. Fish and Wildlife Service. <https://doi.org/10.7944/P927I36K>.
- Udell, B. J., B. R. Straw, S. Loeb, K. M. Irvine, W. E. Thogmartin, C. Lausen, J. D. Reichard, et al. 2024a. "Ecosystems-Nabat-FPabund: Software for Fitting False-Positive N Mixture Models Using NABat Mobile Acoustic Data (Version 1.0.0)." U.S. Geological Survey Software Release. <https://doi.org/10.5066/P9R3W0EZ>.
- Udell, B. J., B. R. Straw, S. Loeb, K. M. Irvine, W. E. Thogmartin, C. Lausen, J. D. Reichard, et al. 2024b. "Supplemental Results from: Using Mobile Acoustic Monitoring and False-Positive N-Mixture Models to Estimate Bat Abundance and Population Trends." U.S. Geological Survey Data Release. <https://doi.org/10.5066/P9WYSBBN>.
- Weller, T. J., T. J. Rodhouse, D. J. Neubaum, P. C. Ormsbee, R. D. Dixon, D. L. Popp, J. A. Williams, et al. 2018. "A Review of Bat Hibernacula across the Western United States: Implications for White-Nose Syndrome Surveillance and Management." *PLoS One* 13(10): e0205647.
- Whitaker, J. O., Jr., and S. L. Gummer. 2000. "Population Structure and Dynamics of Big Brown Bats (*Eptesicus fuscus*) Hibernating in Buildings in Indiana." *The American Midland Naturalist* 143(2): 389–396.
- Whitby, M. D., T. C. Carter, E. R. Britzke, and S. M. Bergeson. 2014. "Evaluation of Mobile Acoustic Techniques for Bat Population Monitoring." *Acta Chiropterologica* 16(1): 223–230.
- Wiens, A. M., B. J. Udell, W. E. Thogmartin, B. R. Straw, T. Cheng, W. F. Frick, and B. E. Reichert. 2023. *North American Bat Monitoring Program (NABat) Bayesian Hierarchical Model for Winter Abundance: Predicted Population Estimates (2022 and 2023)*. Reston, VA: USGS data release. <https://doi.org/10.5066/P9L0578M>.
- Wright, W. J., K. M. Irvine, E. S. Almberg, and A. R. Litt. 2020. "Modelling Misclassification in Multi-Species Acoustic Data when Estimating Occupancy and Relative Activity." *Methods in Ecology and Evolution* 11(1): 71–81.

SUPPORTING INFORMATION

Additional supporting information can be found online in the Supporting Information section at the end of this article.

How to cite this article: Udell, Bradley J., Bethany Rose Straw, Susan C. Loeb, Kathryn M. Irvine, Wayne E. Thogmartin, Cori L. Lausen, Jonathan D. Reichard, et al. 2024. "Using Mobile Acoustic Monitoring and False-Positive N-Mixture Models to Estimate Bat Abundance and Population Trends." *Ecological Monographs* 94(4): e1617. <https://doi.org/10.1002/ecm.1617>